Technical Report No. 2

# SPECIAL STUDIES OF AROD SYSTEM CONCEPTS AND DESIGNS

Contract NAS 8-20128

October 15, 1966

Prepared for

National Aeronautics and Space Administration
George C. Marshall Space Flight Center
Huntsville, Alabama 35812

Author

D. Bradley Crow

Approved by Steven M. Sussman
Steven M. Sussman
Director of Research

Submitted by

ADCOM, Inc.
808 Memorial Drive
Cambridge, Massachusetts 02139

# TABLE OF CONTENTS

# LIST OF ILLUSTRATIONS

## LIST OF ILLUSTRATIONS (Cont.)

# 1. INTRODUCTION AND SUMMARY

This report constitutes the Second Technical Report on the results of a program of investigations carried out by ADCOM, Inc. under Contract No. NAS 8-20128 for George C. Marshall Space Flight Center, Huntsville, Alabama. The specific subject of this report is the Airborne Ranging and Orbit Determination (AROD) Ground Station Antenna and Direction-Finding System. The work on this report was conducted in close coordination with, and in direct support of, the Astrionics Division, George C. Marshall Space Flight Center.

The overall objective of the program is to investigate signaling and signal processing techniques for the AROD system that will most simply and effectively yield unambiguous range and range-rate measurements, within the limitations of existing sources of error, and in harmony with other vehicle and ground station instrumentation functions. The result of the investigations will aid NASA in the planning, design, and implementation of the AROD tracking system.

The primary objectives of this report are:

(a) To analyze the performance of the proposed Ground Station Antenna and D/F System, particularly with respect to system noise and hardware limitations.

(b) To identify any deficiencies in the proposed design which would prohibit the system from meeting any of its performance objectives, and

(c) To propose, wherever practicable, design modifications or changes which would result in improved system performance, reduced complexity, etc.

An analysis of Direction-Finding (D/F) System accuracy as related to gain and phase irregularities in one of the system preamplifiers is undertaken in Chapter 2. The equations for system derivation of the signals representing the angular direction of the VHF transmission are first reviewed.

A gain error is then applied to one of the preamplifier channels in the D/F system Z ring, and the resulting system phase measurement error determined. (The phase measurement error ultimately affects the accuracy of S-band antenna steering.) The simplifying approximation is made that the VHF antenna mutual impedances are zero, and graphs are plotted showing the system phase measurement error as a function of the assumed preamplifier gain error.

An assumed phase error is then inserted in one of the Z ring preamplifiers and the analysis process repeated: the system phase measurement error is computed as a function of the assumed phase error in the Z ring preamplifier. Again the simplifying assumption is made that the mutual impedances in the VHF antenna are zero, and graphs are plotted showing the relationship between system phase measurement error and the phase error in one Z ring preamplifier.

In Chapter 3, estimates of signal and noise levels in the system are computed. The minimum input signal level required for proper operation of the D/F system, and the maximum distance over which the initial design D/F system will operate, are first calculated. The amplitude detectors facilitating selection of either Z or XY rings are then examined, and their inadequacy discussed.

Continuing in Chapter 3, the phase meter "threshold" is examined, such threshold being defined as that input signal-to-noise ratio at which the phase meter output becomes unreliable due to noise. A test is described which was performed on the phase meter to be used in the system, and a graph interpreting the test results is presented.

The results of the investigation of two other subsystem components are also reported in Chapter 3. Tests are described for each of these equipments, and the test results interpreted. In tests performed on the proposed

amplifier-limiters, the differential phase characteristics were found to vary widely, both as a function of the absolute signal level into the two amplifier-limiters, and as a function of the difference in input signal level between the two devices, one input being held constant. The absence of any limiting was found to occur over most of the input dynamic range of the amplifier-limiters. The test results pointed toward the questionable suitability of these components for the use intended. Tests on reactive (passive) multicouplers showed them to be suitable as signal splitting and summing devices. Isolation between ports of the multicouplers was found to be adequate, and provided the multicouplers can be included in the calibration scheme, little error is expected to be introduced into the system through their use.

In Chapter 4, various direction-finding receiver techniques are discussed which are intended to overcome some of the basic shortcomings of the D/F receiver proposed in References 1 and 2. Two fundamental receiver designs are presented, both of which utilize local oscillator signals from the Station Control Receiver for removal of doppler. Several methods of achieving the narrow noise bandwidth required of the D/F receiver are presented, included in which are phase-locked loops used as filters, and conventional filters. Acquisition time of phase-locked loops (including both frequency and phase lock times) is considered, as is derivation of AGC voltages. A brief survey of the various types of conventional filters considered for use in the system is included.

## 2. ANALYSIS OF D/F SYSTEM ACCURACY

### 2.1 Direction-Finding System Operation

A pictorial diagram of the AROD VHF ground system antenna suggested by Auburn University[1,2] is shown in Fig. 2.1. The antenna array is comprised of two "rings": a set of four vertical elements called the Z ring, and a set of four horizontal elements called the XY ring. The outputs from these elements are combined in such a manner as to provide an omnidirectional pattern for operation of the Station Control Receiver, as well as several other "patterns" for the direction finding (D/F) system.

The function of the D/F system is to provide steering information to direct the S-band tracking link antennas. This is done by derivation of two directional cosine analogs – $\ell$ and m – which represent the angular direction from which the VHF transmitting source is radiating. The coordinate system showing the relationships between the angles and $\ell$ and m information is depicted in Fig. 2.2.

The block diagram of the D/F system proposed by Auburn University is shown in Fig. 2.3. Each element from the array of Fig. 2.1 is coupled to a separate preamplifier. Thence, by power division, phase delay (through coaxial transmission lines), and recombination, three signals are derived; a reference signal $V^{(0)}$ (REF), and two signals $K_Z e^{jc\ell}$ and $K_Z e^{jcm}$ (the first containing $\ell$ phase information, the second containing m) whose phases with respect to the reference phase describe $\theta_x$ and $\theta_y$. These signals are amplified and amplitude limited, then converted to a lower frequency for phase comparison. Phase comparison of $\ell$ and m signals to the reference takes place in the phase meter, which converts the phase information to analog voltage form. The two analog voltages, derived sequentially by phase comparison of the two RF signals to the reference, are used ultimately to control electronically steered, S-band phased arrays. These S-band arrays radiate and receive the tracking link signals from the AROD ground station equipment.

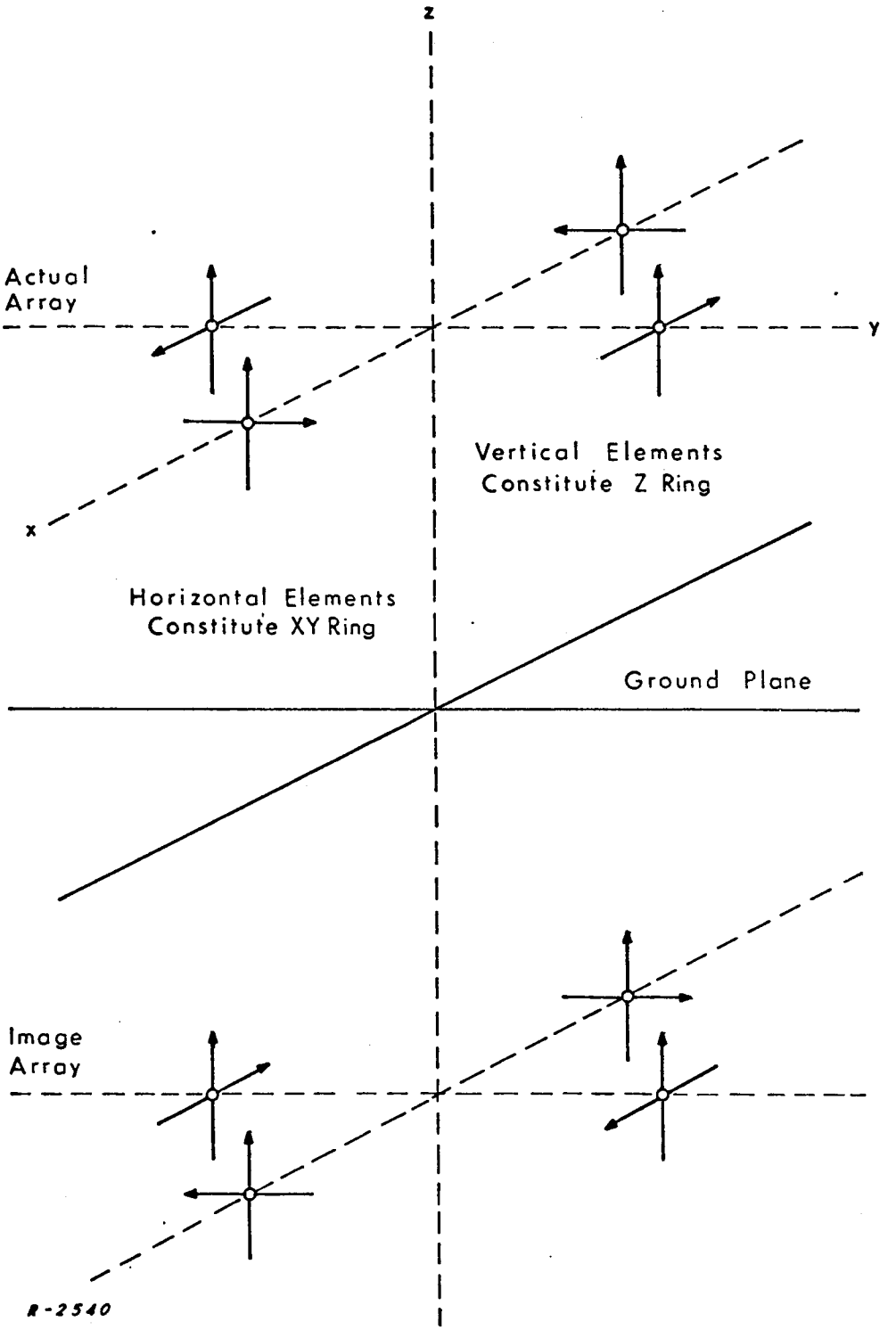


Fig. 2.1 The D/F Antenna and Its Image.

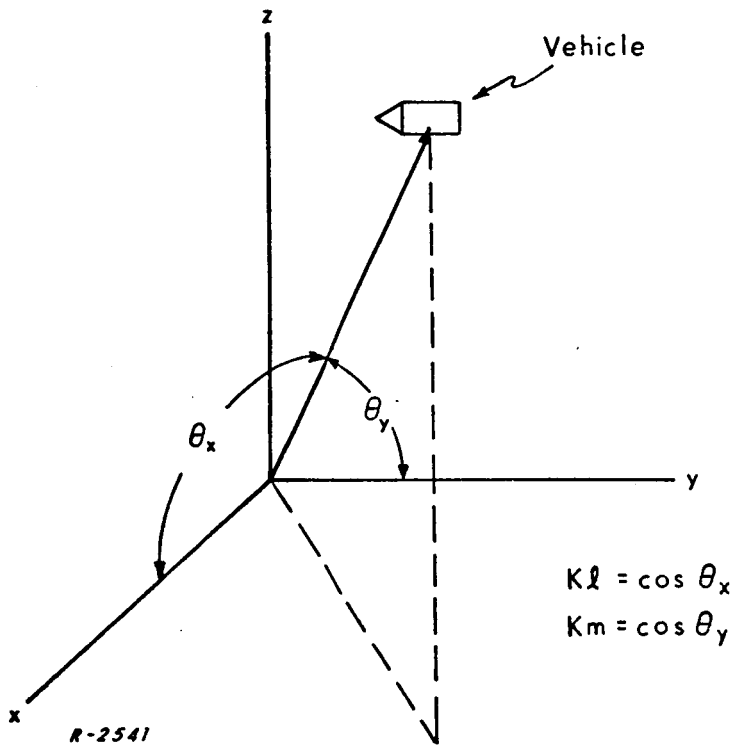


Fig. 2.2 The Coordinate System.

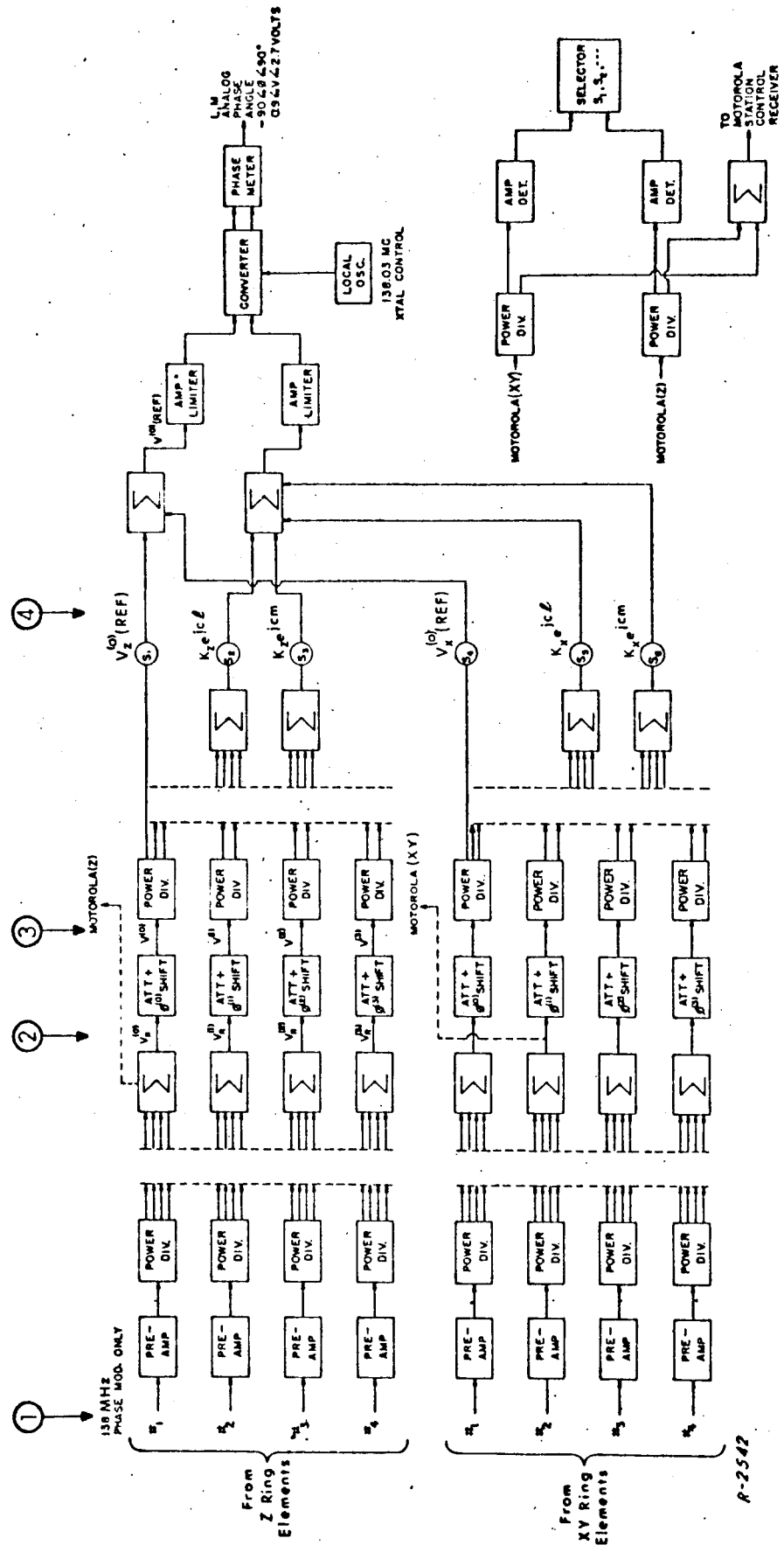


Fig. 2.3 The VHF Direction-Finding System (from Ref. 1).

Mathematically, the direction indication quantities $\ell$ and m are involved in the following four simultaneous equations, representing the antenna element terminal voltages (point ① in Fig. 2.3)

$$Ve^{-jc\ell} = I_1 Z_{11} + I_2 Z_{12} + I_3 Z_{13} + I_4 Z_{12} \tag{2.1}$$

$$Ve^{-jcm} = I_1 Z_{12} + I_2 Z_{11} + I_3 Z_{12} + I_4 Z_{13} \tag{2.2}$$

$$Ve^{jc\ell} = I_1 Z_{13} + I_2 Z_{12} + I_3 Z_{11} + I_4 Z_{12} \tag{2.3}$$

$$Ve^{jcm} = I_1 Z_{12} + I_2 Z_{13} + I_3 Z_{12} + I_4 Z_{11} \tag{2.4}$$

where $I_i$ is the current from the $i^{th}$ dipole; $Z_{11}$ is the self-impedance of each dipole plus the input impedance of the transmission line; $Z_{12}$ is the mutual impedance between two dipoles spaced $\frac{\sqrt{2}\lambda}{4}$ apart; $Z_{13}$ is the mutual impedance between two dipoles spaced $\frac{\lambda}{2}$ apart; c is a constant, and V is proportional to the amplitude of the received signal.

Equations (2.1), (2.2), (2.3), and (2.4) can be solved for $I_1$, $I_2$, $I_3$, and $I_4$ as follows

$$I_1 = V\left[Y_{11}e^{-jc\ell} - Y_{12}e^{-jcm} + Y_{13}e^{jc\ell} - Y_{12}e^{jcm}\right] \tag{2.5}$$

$$I_2 = V\left[-Y_{12}e^{-jc\ell} + Y_{11}e^{-jcm} - Y_{12}e^{jc\ell} + Y_{13}e^{jcm}\right] \tag{2.6}$$

$$I_3 = V\left[Y_{13}e^{-jc\ell} - Y_{12}e^{-jcm} + Y_{11}e^{jc\ell} - Y_{12}e^{jcm}\right] \tag{2.7}$$

$$I_4 = V\left[-Y_{12}e^{-jc\ell} + Y_{13}e^{-jcm} - Y_{12}e^{jc\ell} + Y_{11}e^{jcm}\right] \tag{2.8}$$

where

$$Y_{11} = \frac{Z_{11}^3 + 2Z_{12}^2 Z_{13} - Z_{13}^2 Z_{11} - 2Z_{11}Z_{12}^2}{\Delta} \tag{2.9}$$

$$Y_{12} = \frac{Z_{11}^2 Z_{12} + Z_{12}Z_{13}^2 - 2Z_{11}Z_{12}Z_{13}}{\Delta} \tag{2.10}$$

$$Y_{13} = \frac{2Z_{11}Z_{12}^2 + Z_{13}^3 - 2Z_{12}^2 Z_{13} - Z_{12}Z_{11}^2}{\Delta} \tag{2.11}$$

and

$$\Delta = Z_{11}^4 + Z_{13}^4 - 4Z_{11}^2 Z_{12}^2 - 4Z_{12}^2 Z_{13}^2 - 2Z_{13}^2 Z_{11}^2 + 8Z_{11}Z_{12}^2 Z_{13} \tag{2.12}$$

Following preamplification, power division, phase delay (again through appropriate lengths of transmission line), and summation, the following quantities are developed at point ② in Fig. 2.3

$$V_R^{(0)} = (I_1 + I_2 + I_3 + I_4)R \tag{2.13}$$

$$V_R^{(1)} = (I_1 + jI_2 - I_3 - jI_4)R \tag{2.14}$$

$$V_R^{(2)} = (I_1 - I_2 + I_3 - I_4)R \tag{2.15}$$

$$V_R^{(3)} = (I_1 - jI_2 - I_3 + jI_4)R \tag{2.16}$$

where R is the common load of the four elements.

Substituting Eqs. (2.5) through (2.8) in Eqs. (2.13) through (2.16) yields

$$V_R^{(0)} = VR(Y_{11} - 2Y_{12} + Y_{13})(e^{-jc\ell} + e^{-jcm} + e^{jc\ell} + e^{jcm}) \tag{2.17}$$

$$V_R^{(1)} = VR(Y_{11} - Y_{13})(e^{-jc\ell} + je^{-jcm} - e^{jc\ell} - je^{jcm}) \tag{2.18}$$

$$V_R^{(2)} = VR(Y_{11} + 2Y_{12} + Y_{13})(e^{-jc\ell} - e^{-jcm} + e^{jc\ell} - e^{jcm}) \tag{2.19}$$

$$V_R^{(3)} = VR(Y_{11} - Y_{13})(e^{-jc\ell} - je^{-jcm} - e^{jc\ell} + je^{jcm}) \tag{2.20}$$

Normalization of Eqs. (2.17) through (2.20) through the use of attenuators and phase shifters yields the following signal values at point ③ in Fig. 2.3

$$V^{(0)} = \frac{V_R^{(0)}}{N_0} = e^{-jc\ell} + e^{-jcm} + e^{jc\ell} + e^{jcm} \tag{2.21}$$

$$V^{(1)} = \frac{V_R^{(1)}}{N_1} = e^{-jc\ell} + je^{-jcm} - e^{jc\ell} - je^{jcm} \tag{2.22}$$

$$V^{(2)} = \frac{V_R^{(2)}}{N_2} = e^{-jc\ell} - e^{-jcm} + e^{jc\ell} - e^{jcm} \tag{2.23}$$

$$V^{(3)} = \frac{V_R^{(3)}}{N_1} = e^{-jc\ell} - je^{-jcm} - e^{jc\ell} + je^{jcm} \tag{2.24}$$

where

$$N_0 = VR(Y_{11} - 2Y_{12} + Y_{13}) \tag{2.25}$$

$$N_1 = VR(Y_{11} - Y_{13}) \tag{2.26}$$

$$N_2 = VR(Y_{11} + 2Y_{12} + Y_{13}) \tag{2.27}$$

Following the normalization process, the signals are again power divided, phase delayed (through $\frac{n\lambda}{4}$ segments of transmission line), and recombined to yield the following direction information (at point ④ in Fig. 2.3)

$$V_1 = V^{(0)} + jV^{(1)} - V^{(2)} - jV^{(3)}$$
$$= 4\,e^{jcm} \tag{2.28}$$

$$V_2 = V^{(0)} - V^{(1)} + V^{(2)} - V^{(3)}$$
$$= 4\,e^{jc\ell} \tag{2.29}$$

The phases of Eqs. (2.28) and (2.29) with respect to that of the reference, Eq. (2.21), are then measured in the phase meter to obtain the S-band antenna steering information.

The above procedure is feasible if the four preamplifiers have exactly the same amplification factor and phase shift. If other than this condition exists, however, a notable error in determination of the quantities $\ell$ and $m$ may occur.

## 2.2 Effect of Input Gain Error

Suppose three preamplifiers in the Z ring have identical gains A, and the fourth has gain $A(1+\epsilon)$. Then, from Eqs. (2.13) and (2.21)

$$V'^{(0)} = \frac{R}{N_0}\left[I_1 + I_2 + I_3 + (1+\epsilon)I_4\right] \tag{2.30}$$

Substituting Eqs. (2.5) through (2.8) into Eq. (2.30) and expanding

$$V'^{(0)} = (e^{-jc\ell} + e^{jc\ell} + e^{-jcm} + e^{jcm}) - \frac{\epsilon}{y_o}\left[Y_{12}(e^{-jc\ell} + e^{jc\ell}) - Y_{13}e^{-jcm} - Y_{11}e^{jcm}\right] \tag{2.31}$$

where

$$y_o = Y_{11} - 2Y_{12} + Y_{13} \tag{2.32}$$

By similar substitution and expansion

$$V'^{(1)} = (e^{-jc\ell} - e^{jc\ell} + je^{-jcm} - je^{jcm}) + j\frac{\epsilon}{y_1}\left[Y_{12}(e^{-jc\ell} + e^{jc\ell}) - Y_{13}e^{-jcm} - Y_{11}e^{jcm}\right] \tag{2.33}$$

$$V'^{(2)} = (e^{-jc\ell} + e^{jc\ell} - e^{-jcm} - e^{jcm}) + \frac{\epsilon}{y_2}\left[Y_{12}(e^{-jc\ell} + e^{jc\ell}) - Y_{13}e^{-jcm} - Y_{11}e^{jcm}\right] \tag{2.34}$$

$$V'^{(3)} = (e^{-jc\ell} - e^{jc\ell} - je^{-jcm} + je^{jcm}) - j\frac{\epsilon}{y_1}\left[Y_{12}(e^{-jc\ell} + e^{jc\ell}) - Y_{13}e^{-jcm} - Y_{11}e^{jcm}\right] \tag{2.35}$$

where

$$y_1 = Y_{11} - Y_{13}, \text{ and} \tag{2.36}$$

$$y_2 = Y_{11} + 2Y_{12} + Y_{13} \tag{2.37}$$

Substituting Eqs. (2.31) and (2.33) through (2.35) in Eqs. (2.28) and (2.29) and expanding

$$V_1' = 4e^{jcm} - \epsilon\left[\frac{1}{y_o} + \frac{2}{y_1} + \frac{1}{y_2}\right]\left[Y_{12}(e^{-jc\ell} + e^{jc\ell}) - Y_{13}e^{-jcm} - Y_{11}e^{jcm}\right] \tag{2.38}$$

$$Y_2' = 4e^{jc\ell} - \epsilon\left[\frac{1}{y_o} - \frac{1}{y_2}\right]\left[Y_{12}(e^{-jc\ell} + e^{jc\ell}) - Y_{13}e^{-jcm} - Y_{11}e^{jcm}\right] \tag{2.39}$$

Under the simplifying assumption that $Y_{12} = Y_{13} = 0$,* Eqs. (2.31), (2.38), and (2.39) become

$$V'^{(0)} \approx e^{-jc\ell} + e^{-jcm} + e^{jc\ell} + e^{jcm} + \epsilon\, e^{jcm} \tag{2.40}$$

$$V_1' \approx 4(1 + \epsilon)\, e^{jcm} \tag{2.41}$$

$$V_2' \approx 4e^{jc\ell} \tag{2.42}$$

It is seen from Eqs. (2.41) and (2.42) that the phase angles of $V_1$ and $V_2$ are not affected by an amplitude error in the fourth channel preamplifier.

---

* It is recognized that this approximation is a very gross one. Computation of $V^{(0)}$, $V_1$, and $V_2$ utilizing the actual values of $Y_{12}$ and $Y_{13}$ will likely result in phase measurement errors slightly greater than those computed in this report.

The reference signal does acquire a phase error $\sigma$, however, which is

$$\sigma = \tan^{-1}\left[\frac{\epsilon \tan cm}{2\,\frac{\cos c\ell}{\cos cm} + 2 + \epsilon}\right] \tag{2.43}$$

The measurement phase error $\rho$ is

$$\rho = -\sigma \tag{2.44}$$

Phase measurement error $\rho$ is plotted against preamplifier gain error $\epsilon$ for various values of cm in Fig. 2.4a for $c\ell = 0$, and in Fig. 2.4b for $c\ell = \pm 90$ degrees. Note from Fig. 2.4b that very large errors (up to 90 degrees) can be obtained, even with very small values of $\epsilon$ when both $c\ell$ and cm are large.

## 2.3 Effect of Input Phase Error

Now suppose three preamplifiers in the Z ring have identical phase delays and the fourth has a relative phase shift error $\delta$ associated with it. Then, from Eqs. (2.13) and (2.21)

$$V''(0) = \frac{R}{N_0}\left[I_1 + I_2 + I_3 + I_4 e^{j\delta}\right] \tag{2.45}$$

Substituting Eqs. (2.5) through (2.8) into Eq. (2.45) and expanding

$$\begin{aligned} V''(0) = {} & e^{-jc\ell} + e^{jc\ell} + e^{-jcm} + e^{jcm} \\ & + \left(\frac{Y_{12} - Y_{12}e^{j\delta}}{y_o}\right)e^{-jc\ell} + \left(\frac{Y_{12} - Y_{12}e^{j\delta}}{y_o}\right)e^{jc\ell} \\ & - \left(\frac{Y_{13} - Y_{13}e^{j\delta}}{y_o}\right)e^{-jcm} - \left(\frac{Y_{11} - Y_{11}e^{j\delta}}{y_o}\right)e^{jcm} \end{aligned} \tag{2.46}$$

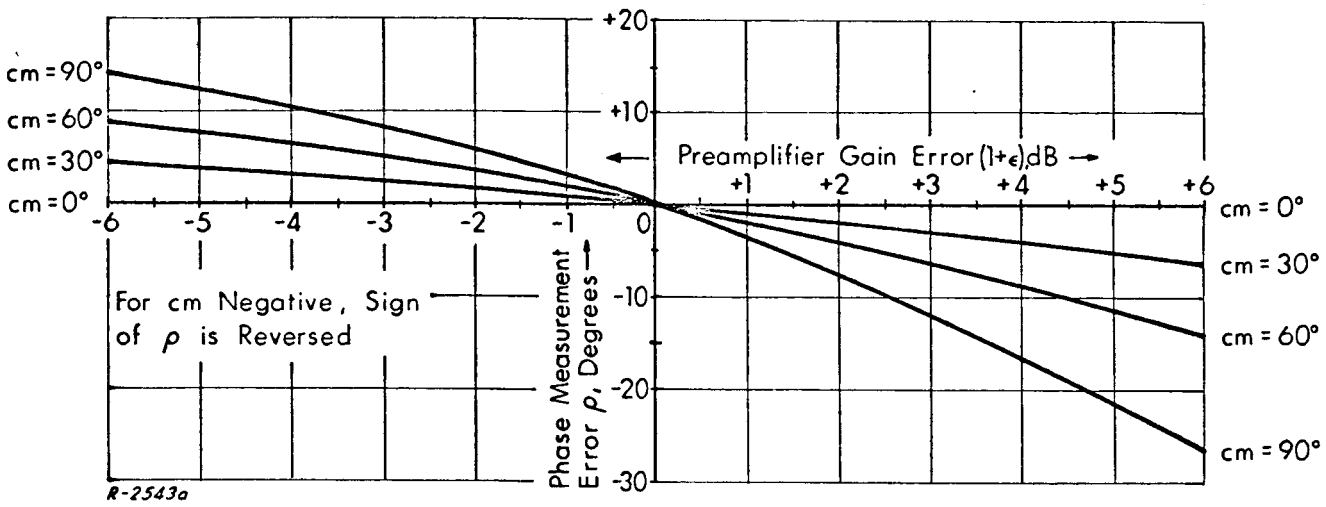


Fig. 2.4a Error in Phase Measurement due to Preamplifier Gain Error, $c\ell = 0^{o}$

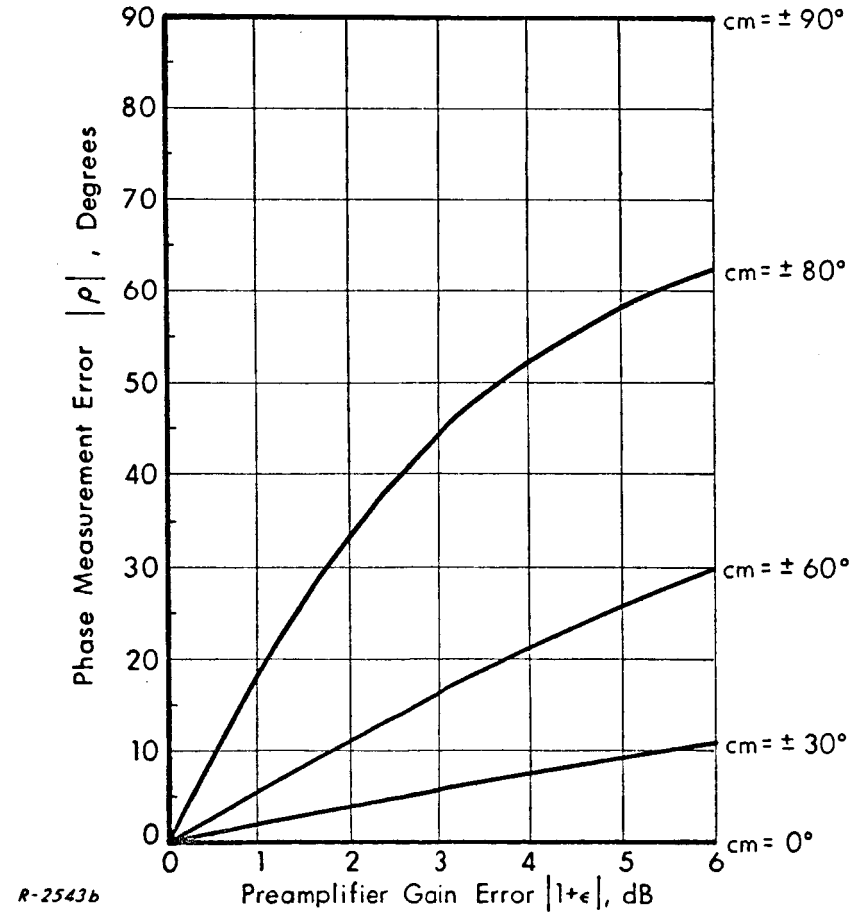


Fig. 2.4b Error in Phase Measurement due to Preamplifier Gain Error, $c\ell = \pm 90^{o}$

By similar substitution and expansion

$$V''(1) = e^{-jc\ell} - e^{jc\ell} + j(e^{-jcm} - e^{jcm}) - j\left(\frac{Y_{12} - Y_{12}e^{j\delta}}{y_1}\right)e^{-jc\ell} - j\left(\frac{Y_{12} - Y_{12}e^{j\delta}}{y_1}\right)e^{jc\ell} + j\left(\frac{Y_{13} - Y_{13}e^{j\delta}}{y_1}\right)e^{-jcm} + j\left(\frac{Y_{11} - Y_{11}e^{j\delta}}{y_1}\right)e^{jcm} \quad (2.47)$$

$$V''(2) = e^{-jc\ell} + e^{jc\ell} - e^{-jcm} - e^{jcm} - \left(\frac{Y_{12} - Y_{12}e^{j\delta}}{y_2}\right)e^{-jc\ell} - \left(\frac{Y_{12} - Y_{12}e^{j\delta}}{y_2}\right)e^{jc\ell} + \left(\frac{Y_{13} - Y_{13}e^{j\delta}}{y_2}\right)e^{-jcm} + \left(\frac{Y_{11} - Y_{11}e^{j\delta}}{y_2}\right)e^{jcm} \quad (2.48)$$

$$V''(3) = e^{-jc\ell} - e^{jc\ell} - j(e^{-jcm} - e^{jcm}) + j\left(\frac{Y_{12} - Y_{12}e^{j\delta}}{y_1}\right)e^{-jc\ell} + j\left(\frac{Y_{12} - Y_{12}e^{j\delta}}{y_1}\right)e^{jc\ell} - j\left(\frac{Y_{13} - Y_{13}e^{j\delta}}{y_1}\right)e^{-jcm} - j\left(\frac{Y_{11} - Y_{11}e^{j\delta}}{y_1}\right)e^{jcm} \quad (2.49)$$

Substituting Eqs. (2.46) through (2.49) into Eqs. (2.28) and (2.29) and expanding

$$V_1'' = 4e^{jcm} + X(e^{-jc\ell} + e^{jc\ell}) - Ye^{-jcm} - Ze^{jcm} \quad (2.50)$$

where

$$X = \left(\frac{Y_{12} - Y_{12}e^{j\delta}}{y_o}\right) + 2\left(\frac{Y_{12} - Y_{12}e^{j\delta}}{y_1}\right) + \left(\frac{Y_{12} - Y_{12}e^{j\delta}}{y_2}\right) \tag{2.51}$$

$$Y = \left(\frac{Y_{13} - Y_{13}e^{j\delta}}{y_o}\right) + 2\left(\frac{Y_{13} - Y_{13}e^{j\delta}}{y_1}\right) + \left(\frac{Y_{13} - Y_{13}e^{j\delta}}{y_2}\right) \tag{2.52}$$

$$Z = \left(\frac{Y_{11} - Y_{11}e^{j\delta}}{y_o}\right) + 2\left(\frac{Y_{11} - Y_{11}e^{j\delta}}{y_1}\right) + \left(\frac{Y_{11} - Y_{11}e^{j\delta}}{y_2}\right) \tag{2.53}$$

and

$$\begin{aligned} V_2'' = 4e^{jc\ell} &+ \left[\left(\frac{Y_{12} - Y_{12}e^{j\delta}}{y_o}\right) - \left(\frac{Y_{12} - Y_{12}e^{j\delta}}{y_2}\right)\right] e^{-jc\ell} \\ &+ \left[\left(\frac{Y_{12} - Y_{12}e^{j\delta}}{y_o}\right) - \left(\frac{Y_{12} - Y_{12}e^{j\delta}}{y_2}\right)\right] e^{jc\ell} \\ &+ \left[\left(\frac{Y_{13} - Y_{13}e^{j\delta}}{y_2}\right) - \left(\frac{Y_{13} - Y_{13}e^{j\delta}}{y_o}\right)\right] e^{-jcm} \\ &+ \left[\left(\frac{Y_{11} - Y_{11}e^{j\delta}}{y_2}\right) - \left(\frac{Y_{11} - Y_{11}e^{j\delta}}{y_o}\right)\right] e^{jcm} \end{aligned} \tag{2.54}$$

Under the simplifying assumption that $Y_{12} = Y_{13} = 0$, Eqs. (2.46), (2.50) and (2.54) become

$$V''(0) \approx e^{-jc\ell} + e^{jc\ell} + e^{-jcm} + e^{j(cm+\delta)} \tag{2.55}$$

$$V_1'' \approx 4\, e^{j(cm + \delta)} \tag{2.56}$$

$$V_2'' \approx 4\, e^{jc\ell} \tag{2.57}$$

The phase angle $\alpha$ of $V''(0)$ is

$$\alpha \approx \tan^{-1} \frac{\cos(cm + \frac{\delta}{2}) \sin \frac{\delta}{2}}{\cos c\ell + \cos(cm + \frac{\delta}{2}) \cos \frac{\delta}{2}} \tag{2.58}$$

The error in the measurement of the phase of m information is given by

$$\gamma_m = \delta - \alpha \tag{2.59}$$

$\gamma_m$ is plotted against $\delta$ in Fig. 2.5 for various values of $c\ell$ and cm. Note that when $c\ell = \pm 90^\circ$, $\gamma_m$ is independent of the value of cm.

The error in the measurement of the phase of $\ell$ information is given by

$$\gamma_\ell = -\alpha \tag{2.60}$$

$\gamma_\ell$ is plotted against $\delta$ in Fig. 2.6 for various values of $c\ell$ and cm. Note again that when $c\ell = \pm 90^\circ$, $\gamma_\ell$ is independent of the value of cm.

## 2.4 Conclusions

From the above analysis, we can conclude that the D/F system is relatively sensitive to gain and phase variations in the system RF preamplifiers. Even under the ideal condition of no mutual coupling between elements of the antenna, there are errors due to RF preamplifier gain and phase differences.

It is recommended that serious consideration be given to the tradeoffs involved in development of RF preamplifiers to meet the desired gain and phase stability requirements versus the degradation in system performance which would occur were the preamplifiers to be eliminated from the system entirely.

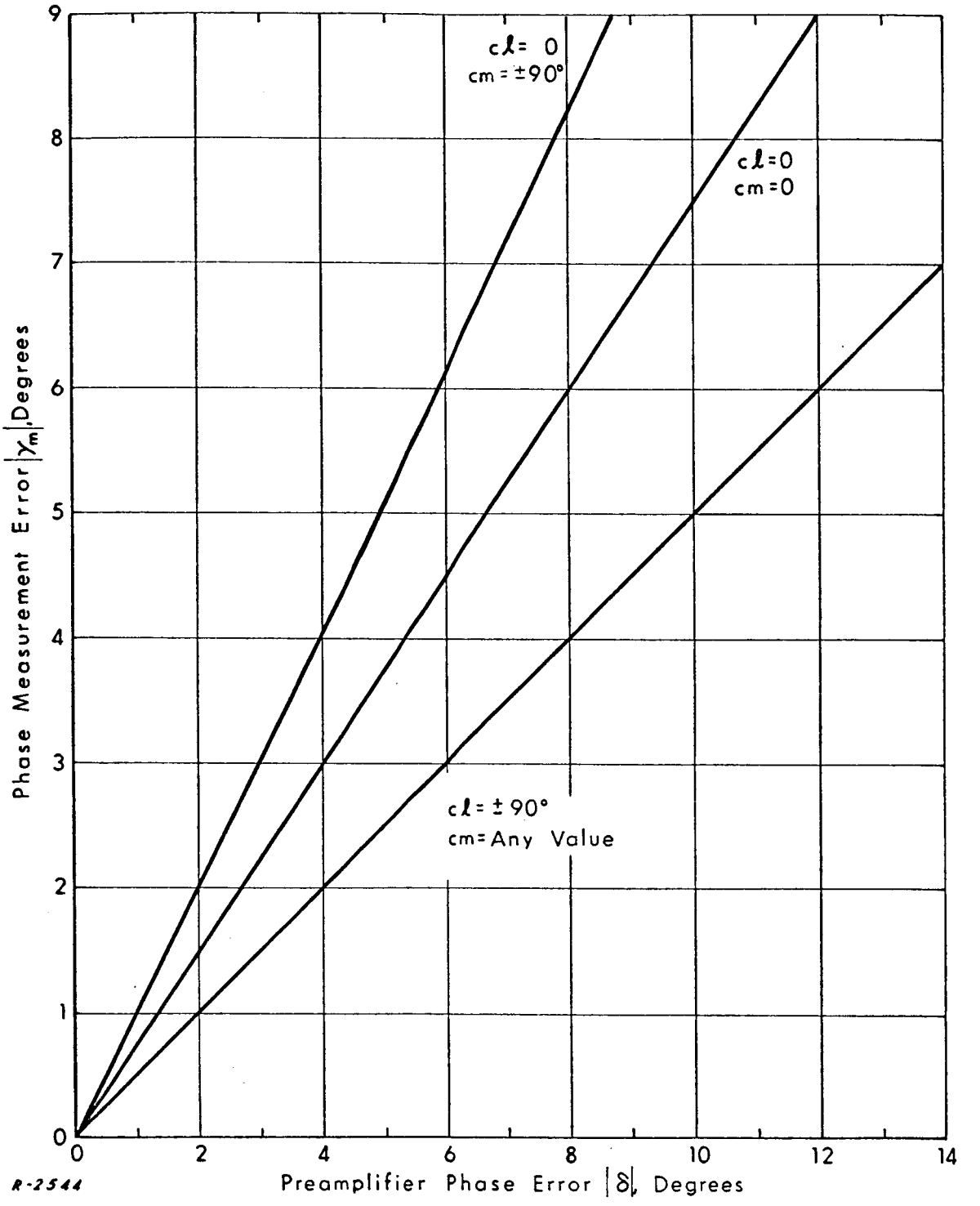


Fig. 2.5 m Information Phase Error Resulting from Preamplifier Phase Error δ.

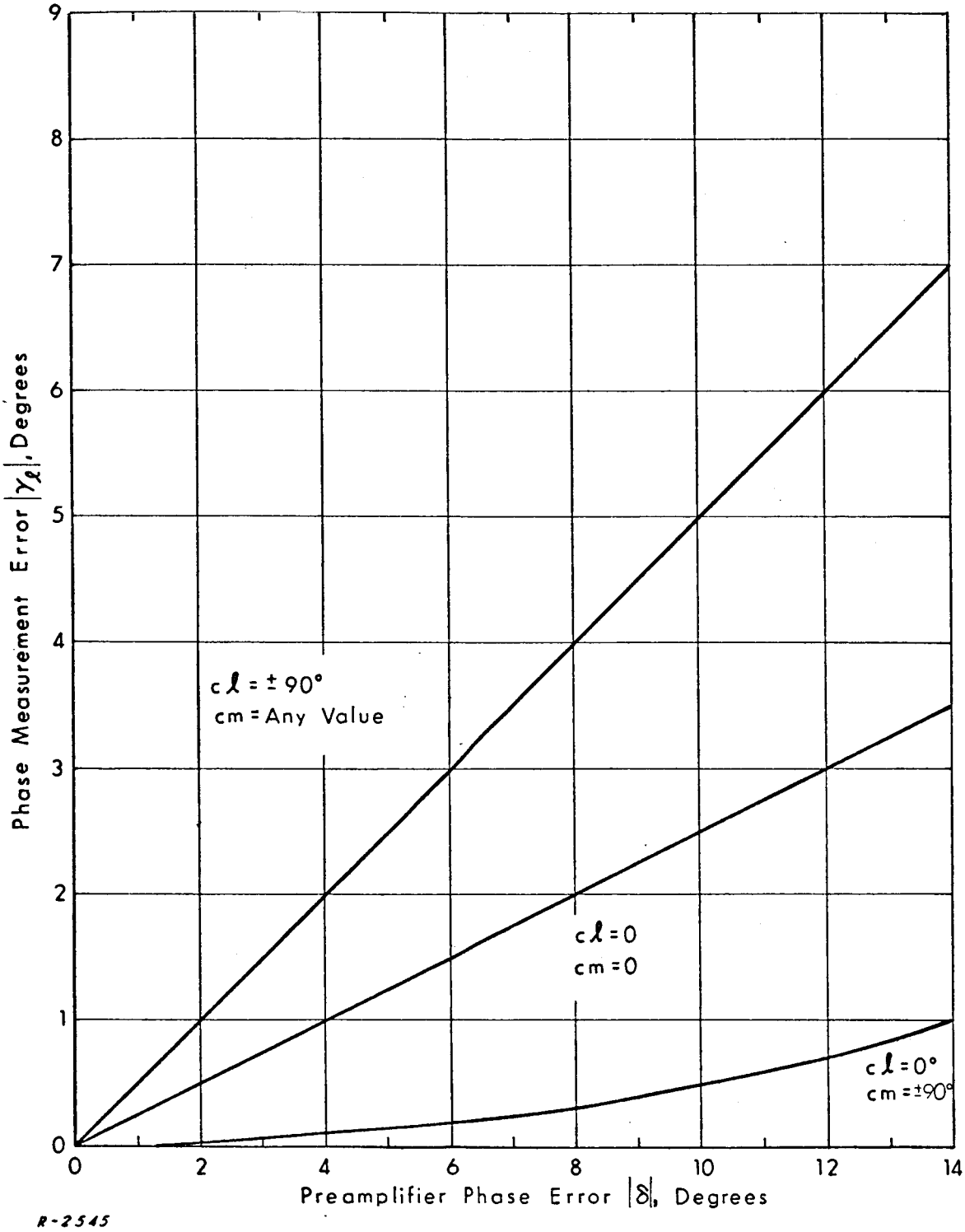


Fig. 2.6 $\underline{\ell}$ Information Phase Error Resulting from Preamplifier Phase Error $\delta$.

# 3. ANALYSIS OF D/F SYSTEM PERFORMANCE

In this chapter a cursory analysis of the performance of the D/F system in the presence of noise is undertaken. In addition, various components of the breadboard system developed by Auburn University[1, 2] are examined for the purpose of determining their suitability for use in the final system. The results of various tests on these components are reported, such tests having been conducted with the cooperation of Auburn University in the period January through March 1966.

## 3.1 D/F Receiver Thresholds

There are two thresholds of special significance in the direction-finding receiver: that of the channels from which the S-band antenna steering signal is derived, and that of the channels providing ring selection criteria to the SELECTOR (see Fig. 2.3). A brief analysis of each is contained in this section.

### 3.1.1 Steering Information Threshold

The noise bandwidth of the phase information carrying channels in the D/F system proposed by Auburn University (see Fig. 2.3) is determined by the frequency converter immediately preceding the phase meter. Each channel of the converter is modified to pass a bandwidth of 190 kHz. System parameters assumed for D/F system threshold calculations are as follows:

Average Sky (Cosmic) Noise Temperature = $1650^{\circ}K$ (3.1)

System Noise Temperature = $350^{\circ}K$ (3.2)

System Noise Density (at $T = 2000^{\circ}K$) = $N_o = -165.6 \frac{dBm}{Hz}$ (3.3)

Phase Information Channel Noise Bandwidth = $B_1 = 190$ kHz (3.4)

Phase Meter Threshold, SNR Each Cannel = $R = +13.0$ dB (3.5)

The minimum input signal level S required for proper operation of the direction-finding system may be represented by

$$(S)_{dBm} = (N_o)_{\frac{dBm}{Hz}} + (B_1)_{dB\,Hz} + (R)_{dB} \qquad (3.6)$$

$$= -165.6 + 52.8 + 13.0$$

$$= -99.8 \text{ dBm} \qquad (3.7)$$

The Station Control Receiver is designed to operate over an input signal dynamic range of -130 dBm to -60 dBm. It will be noted that there is approximately 30.2 dB threshold difference between the VHF Station Control and D/F receivers.

Parameters assumed for calculation of the maximum range at which the D/F receiver will operate are as follows:

$$\text{Transmitter Power} = P_T = +37.8 \text{ dBm} \qquad (3.8)$$

$$\text{Antenna Gain, Polarization and Other Miscellaneous Losses} = G = -8.0 \text{ dB} \qquad (3.9)$$

The signal path loss, L, for proper operation of the D/F receiver, can therefore be no more than

$$(L)_{dB} = -(P_T)_{dBm} - (G)_{dB} + (S)_{dBm} \qquad (3.10)$$

$$= -37.8 + 8.0 - 99.8$$

$$= -129.6 \text{ dB} \qquad (3.11)$$

This path loss corresponds to a distance of 462 km at a carrier frequency of 138 MHz.

### 3.1.2 Ring Selection Thresholds

A noncoherent amplitude detector has been proposed as the circuit which would provide ring selection criteria to the "SELECTOR" (see Fig. 2.3). Presumably pre-detection and post-detection filtering would be employed in a manner similar to that shown in Fig. 3.1.

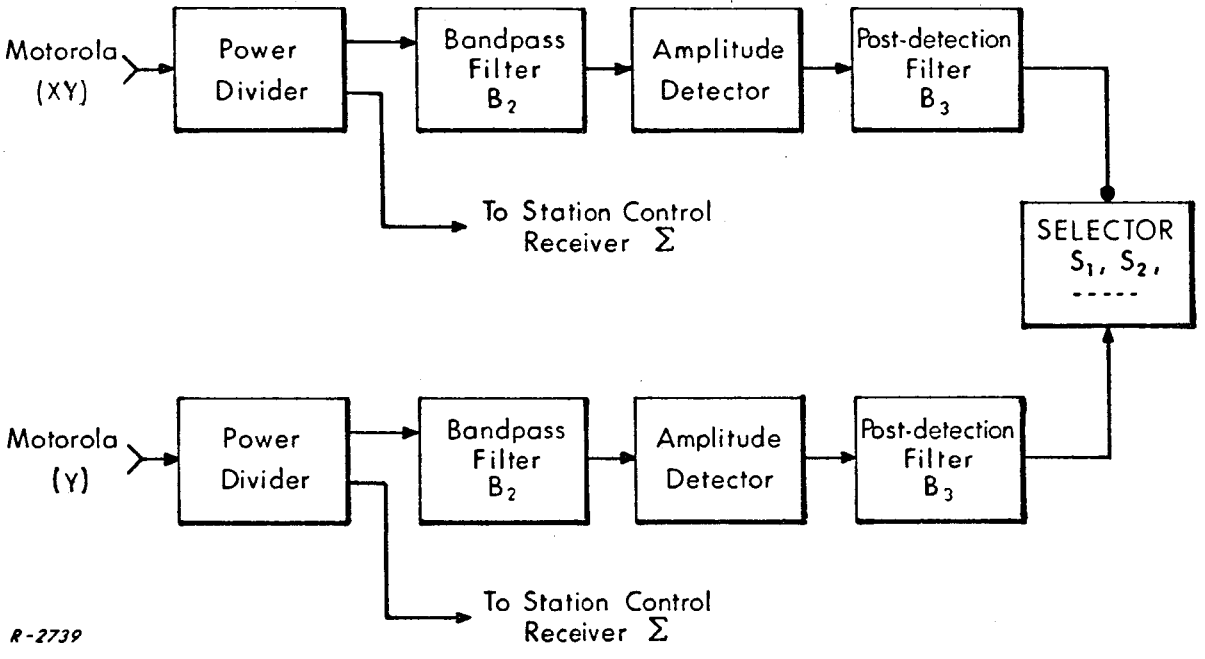


Fig. 3.1 Filtering at Input and Output of Amplitude Detectors.

Hypothesizing a maximum attainable Q of 100 (utilizing conventional bandpass filtering techniques at the carrier frequency -- 138 MHz), the noise bandwidth $B_2$ at the input to the amplitude detector is 1.38 MHz. Assuming a system noise density of $-165.6 \frac{dBm}{Hz}$ and an input power of -130 dBm, the signal-to-noise ratio (SNR) at the input to the amplitude detector is -25.8 dB. For a square law detector,

$$SNR_{out} = (SNR_{in})^2 \qquad (3.12)$$

when $SNR_{in} \ll 0$ dB. With an input SNR of -25.8 dB, the output SNR is therefore -51.6 dB.

From the brief analysis above, it is readily seen that conventional filtering techniques do not provide sufficient noise reduction for noncoherent detection at the carrier frequency.

### 3.1.3 Conclusions

The thresholds of ring selection circuitry, and of the circuitry wherein the S-band antenna steering signal is derived, are not commensurate with the requirement for reliable AROD system operation at a maximum range of 2,000 km.* The D/F receiver depicted in Fig. 2.3 is thus not adequate for input signals of very low level. Alternate D/F receiver designs are discussed in Chapter 4 which permit operation of the D/F system at signal levels consistent with those for which AROD vehicle and ground station tracking equipment is designed.

## 3.2 Phase Meter Threshold

To permit circuit margin calculations on the circuit of Fig. 2.3, it is necessary to know with some measure of certainty the input signal-to-noise ratio (SNR) at which the phase meter output signal becomes unreliable due to noise. Since it was anticipated that any theoretical "threshold" calculations might differ markedly from those obtained in actual operational hardware, it was deemed advisable to determine such threshold characteristics experimentally utilizing the actual equipment proposed for use in the breadboard system.

---

*The design goal for the AROD tracking system (vehicle and ground station equipment) is for a 20 dB signal margin to occur at the maximum specified range of 2,000 km.

### 3.2.1 Threshold Test

The AD-YU model 524A Digital Phase Meter with model 306 Frequency Converter was selected by Auburn University to be used in the circuit of Fig. 2.3. It was felt that the most meaningful threshold test on this device would be one in which errors due to noise could be evaluated in terms of accuracy of the operational system.

As was discussed in Chapter 2, $\ell$ and m information are sampled sequentially so as to require only one phase meter. Lowpass filtering is employed at the phase meter output* to reduce the noise coupled to analog-to-digital (A/D) conversion equipment (used to digitally control S-band antenna steering). The test setup shown in Fig. 3.2 was thus used for the threshold test.

A phase-stable signal from a 138 MHz crystal oscillator was coupled through a step attenuator and power divider to two coaxial transmission lines with lengths $\lambda_1$ and $\lambda_2$. The difference in electrical length of the transmission lines represented approximately 90 degrees at the carrier frequency 138 MHz. The SNR into the digital phase meter was varied during the test by adjustment of the step attenuator following the 138 MHz crystal oscillator. Constant level additive noise was introduced through the amplifier stages of the frequency converter. Signal and noise levels were measured with a wave analyzer and true rms voltmeter, respectively. RMS noise voltage was measured with no input signal present. The narrowband characteristics of the wave analyzer served to filter the noise during signal voltage measurements, thus enabling reliable readings at low signal-to-noise ratios.

A post-detection lowpass filter was employed at the analog output of the phase meter. The filter used was similar to the one which would be used in the breadboard system* so as to simulate actual operating conditions as closely as possible. The time constant $\tau$ of the filter used in the test was approximately 0.3 second.

*See Appendix B

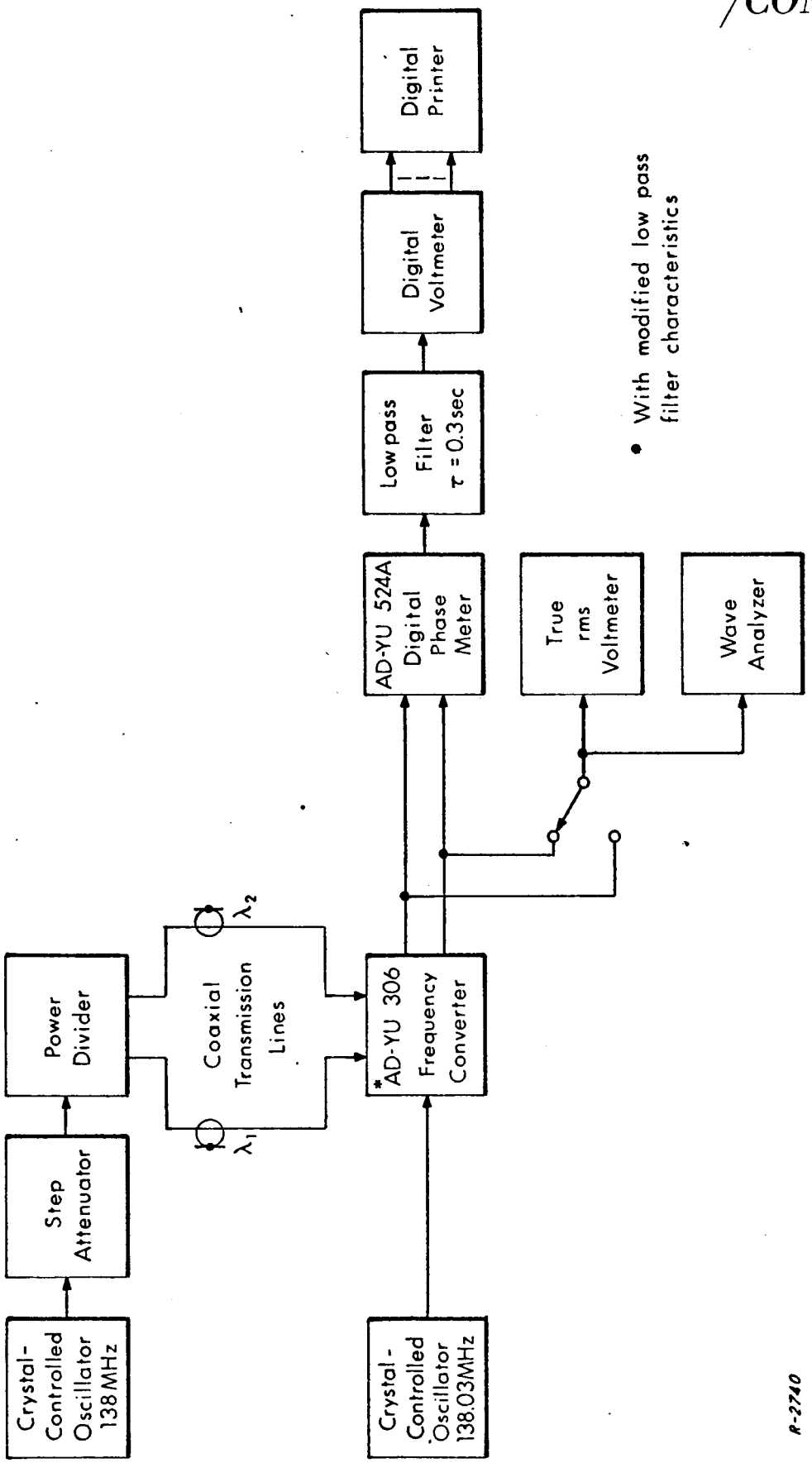


Fig. 3.2 Test Setup for Measurement of Phase Meter Threshold.

The digital voltmeter and digital printer were adjusted to read and print out every one-half second a voltage measurement representing the phase of the input signal. In this manner the test closely duplicated the phase measurement process that would be employed in the breadboard system, and the results could be related meaningfully to the phase measurement error that could be expected due to noise. Fifty phase meter output printouts were taken for each input SNR for which measurements were desired.

The mean value of the fifty readings is plotted in Fig. 3.3 as a function of SNR; the standard deviation of these readings is also plotted. The mean value could reasonably be expected to be constant, regardless of the input SNR. The standard deviation curve is represented approximately as expected. Two explanations are possible for the unexpected departure of the mean curve from that of a constant value:

(1) A bias in phase meter response to noise may have resulted from an unbalance in phase meter circuitry. Such an anomaly could cause the sharp rise in the mean phase reading curve below a SNR of about +8 dB.

(2) The differential phase of the amplifiers in the frequency converter varied slightly as a function of input signal level.* This error is evidenced by the slightly negative slope in the mean phase reading curve above an input SNR of approximately +12 dB. No effort was made to hold the signal level constant at the input to the frequency converter** since, at the signal levels corresponding to the SNR range over which the test was made, no amplitude limiting of the input signal occurs in the operational system.

---

*This hypothesis was subsequently verified by independent test.

**The level of one input signal with respect to the other, however, was always within the 6 dB tolerance required to maintain the specified phase meter accuracy.

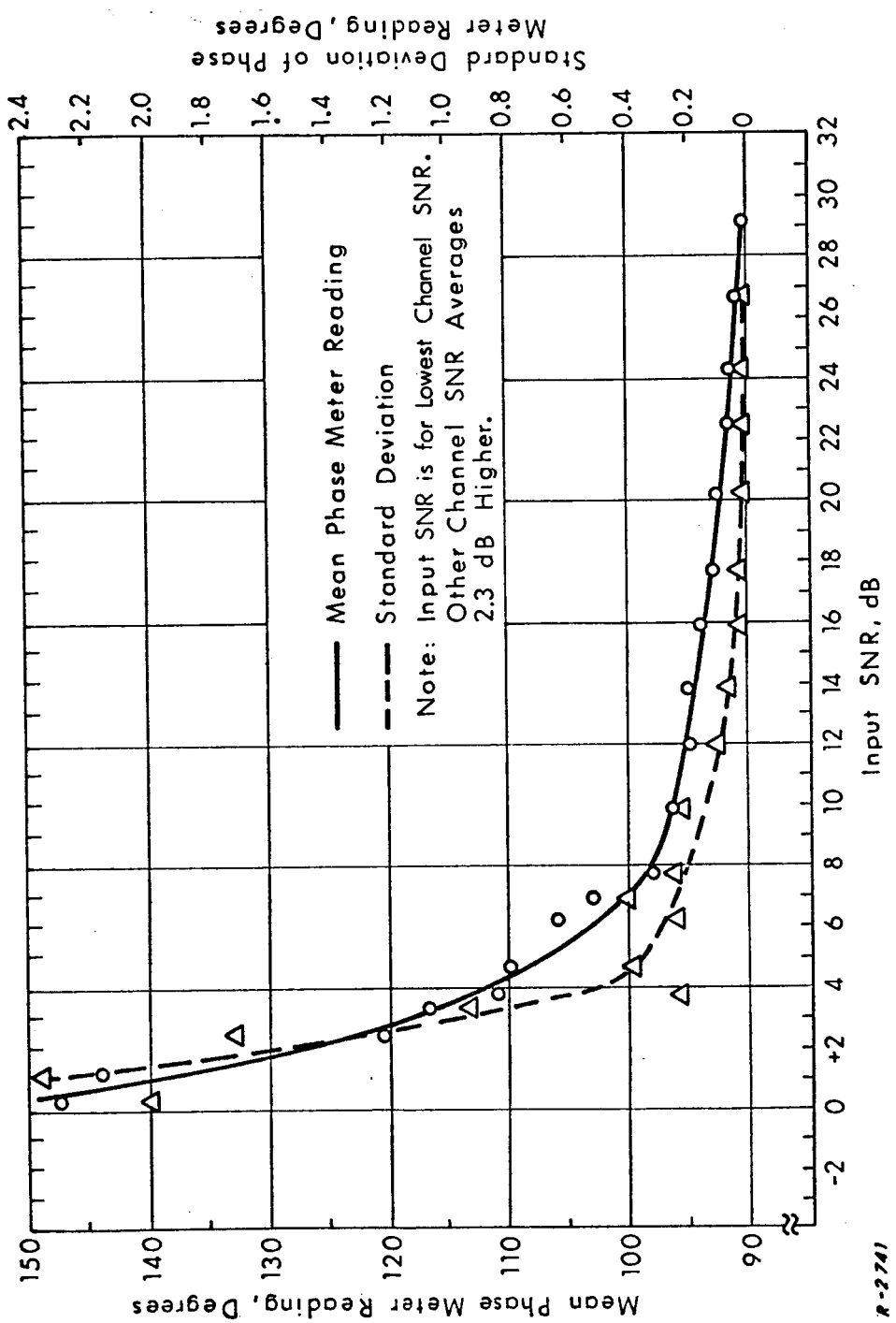


Fig. 3.3 Phase Meter Threshold Curves.

### 3.2.2 Conclusions

Whatever the cause, the errors measured in the test are ones which would be experienced during actual operation of the system. With reference to Fig. 3.3, it will be noted that both curves – mean reading and standard deviation – have rather sharp "knees" beginning at a SNR of about +10 dB. This SNR is the value below which reliable phase meter readings are not obtained due to noise. It will be noted, however, that the departure of the curves from a relatively constant value begins at a SNR of approximately +13 dB. A SNR of +13 dB is thus defined as the "phase meter threshold." This value verifies the phase meter threshold assumed in Eq. (3.5).

## 3.3 Amplifier-Limiters

The use of amplifier-limiters is suggested in References 1 and 2* to supply sufficient signal power at the inputs to the frequency converter, and to ensure that the two input signals are within the required input differential amplitude tolerance for proper operation of the phase meter. The amplifier-limiters chosen were LEL model IF 30-6049, providing a maximum gain of 120 dB.

Any change in the differential phase characteristics between amplifier-limiters as a function of a change in input signal level would result in an S-band antenna steering error. Since amplitude limiting occurs at the carrier frequency – 138 MHz – in References 1 and 2, it was deemed advisable to investigate the differential phase characteristics of the amplifier-limiters as a function

*See Page 31, Reference 1, and page 29, Reference 2.

of input signal level. In addition, it was necessary to know within what amplitude range the two output signals of the amplifier-limiters would fall, assuming input signals of differing levels, to determine whether the specified phase meter accuracy could be met. Several tests were thus performed on the units by Auburn University. Data for graphs contained in this section were supplied by the Auburn University Antenna Research Laboratory.

### 3.3.1 Differential Phase Characteristics

The test setup shown in Fig. 3.4 was employed to measure the phase between two amplifier-limiters as a function of input signal level. For the first test, attenuator $A_2$ was set to zero dB attenuation and input power to both amplifier-limiters varied simultaneously by adjustment of attenuator $A_1$. A series of phase difference readings was thus obtained for various signal levels. A fixed-length coaxial transmission line was inserted prior to one amplifier-limiter to provide a fixed "phase bias" to the phase meter.* The results of this test are shown in Fig. 3.5 for bias levels, $E_b$, of zero, -1, -2, -3, -4, -5, and -6 volts. It will be noted that over the input signal power range (both input signals of equal power) -97 dBm** to -10 dBm, the maximum variation in phase difference readings ranges from 13 degrees to 35 degrees, depending on the amplifier-limiter bias setting. The variation is minimum for a bias setting of $E_b$ = -4 volts.

---

* The AD-YU 524A Digital Phase Meter does not operate reliably when measuring phase values very near zero degrees. The insertion of a coaxial delay line in one input leg of the phase meter facilitates a constant phase offset, thus allowing reliable phase measurements to be made near zero degrees.

** Phase difference readings at input signal levels below approximately -97 dBm are suspected to be unreliable due to noise.

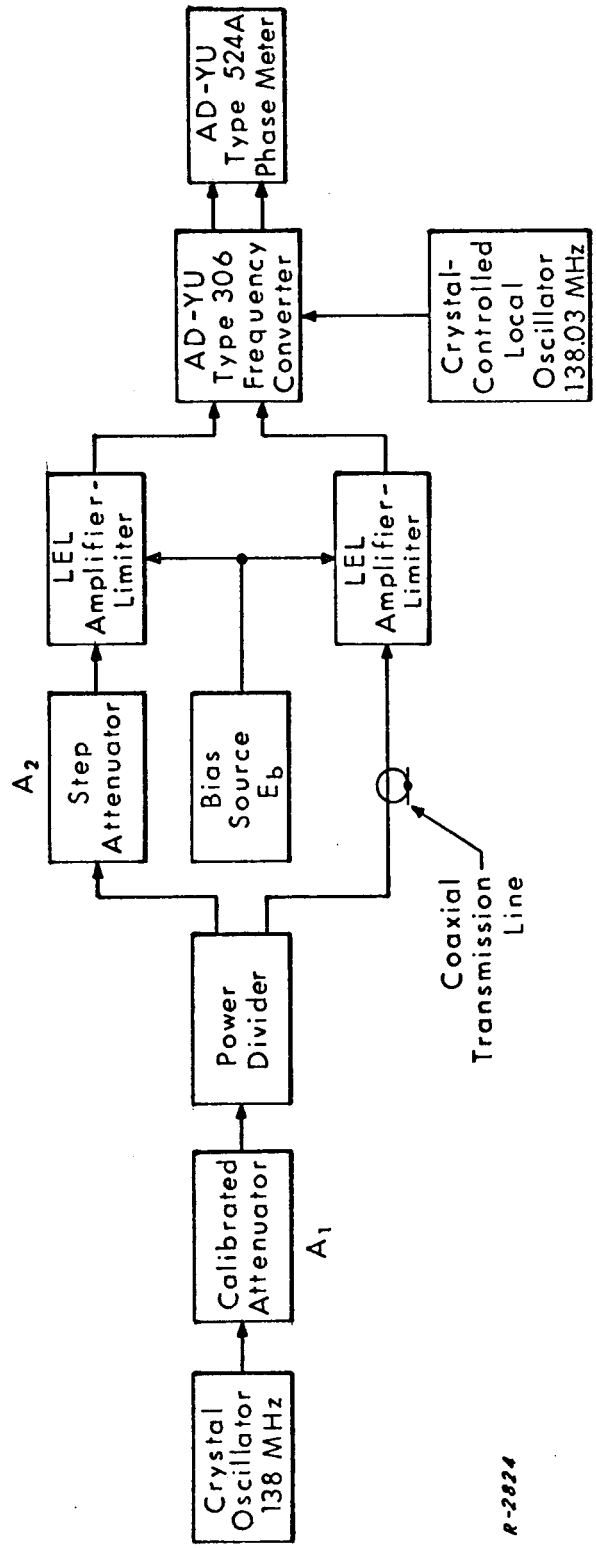


Fig. 3.4 Test Setup for Measurement of Amplifier-Limiter Phase Characteristics.

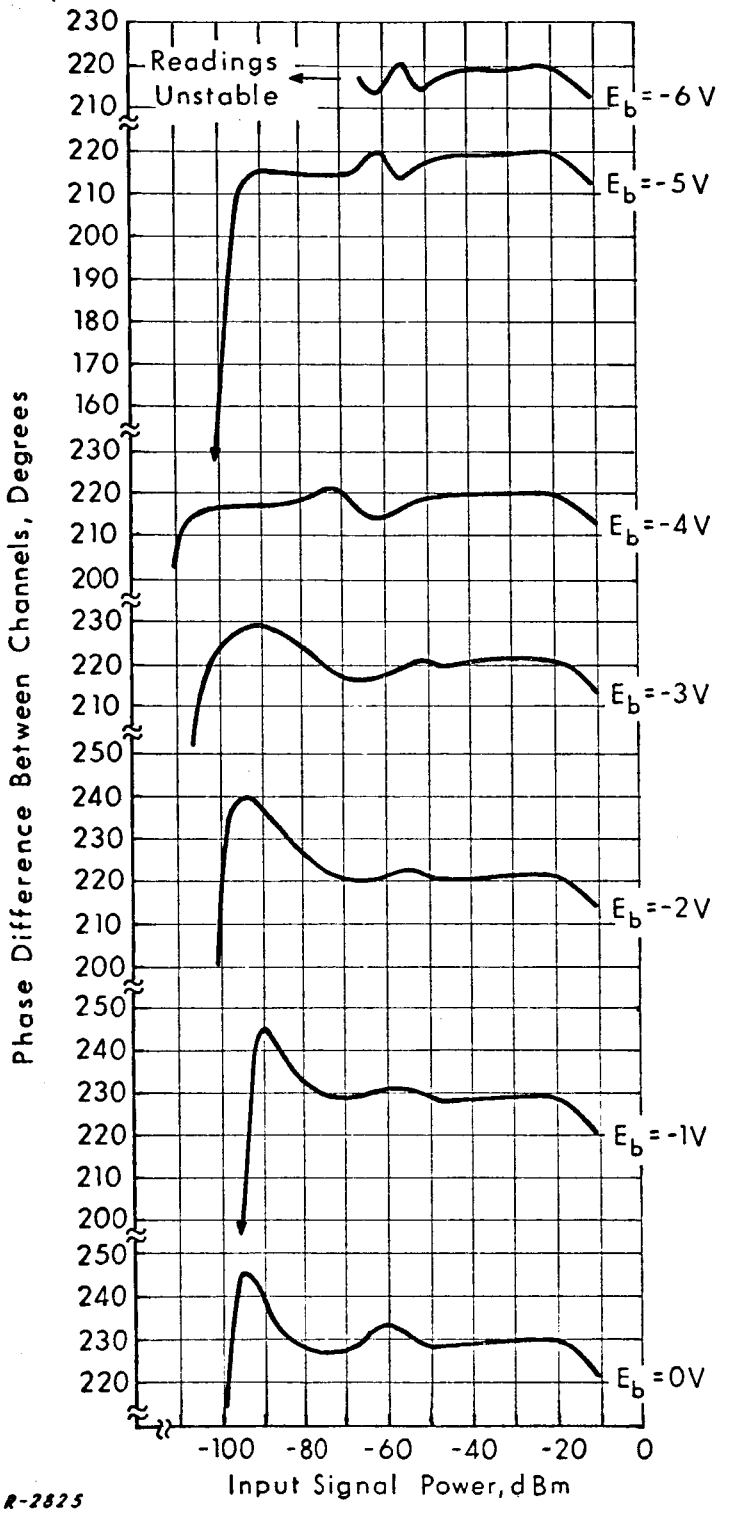


Fig. 3.5 Phase Difference Between Channels as a Function of Input Signal Level.

The likelihood of the input signals to amplifier-limiters being of equal amplitude is not great, since the antenna "patterns" of reference and signal information channels are not identical. The differential phase characteristics of amplifier-limiters as a function of non-equal amplifier-limiter input signal levels was therefore investigated. In this test, the input signal level to one amplifier-limiter was held constant and the input signal level to the other amplifier-limiter was varied by means of adjustment of attenuator $A_2$ (see Fig. 3.4). Phase difference readings were then taken as a function of the input signal amplitude difference. The results of this test are plotted in Fig. 3.6 for a bias setting of $E_b = -5$ volts. Note that a variation in phase difference readings of 14 degrees occurs for an input amplitude difference of 14 dB.

All phase difference readings were taken after the amplifier-limiters had stabilized for a period of 30-45 minutes. Prior to this time, phase readings drifted quite badly.

### 3.3.2 Amplitude Limiting Characteristics

The test setup shown in Fig. 3.7 was employed to determine the output versus input signal power characteristics of the amplifier-limiters (i.e., their amplitude limiting characteristics). The 30 MHz IF amplifier power level indicator was first calibrated over the useful range by coupling the 138 MHz signal generator directly to the crystal mixer input (see amplifier-limiter and calibrated attenuator bypass, Fig. 3.7). Output power readings were then taken on the calibrated IF amplifier for various amplifier-limiter input signal levels. Resulting output power is plotted against input power in Fig. 3.8. Curves for $E_b = 0, -3$, and $-4$ volts are shown. (Curves for $E_b = -1$ and $-2$ volts are not plotted; they are nearly identical to the curve for $E_b = 0$.) It will be noted from Fig. 3.8 that for the $E_b = 4$ volts curve, an amplitude difference in input signals of 14 dB may result in a difference of up to 14 dB between amplifier-limiter output signals. Thus, for a large segment of the range of input signal

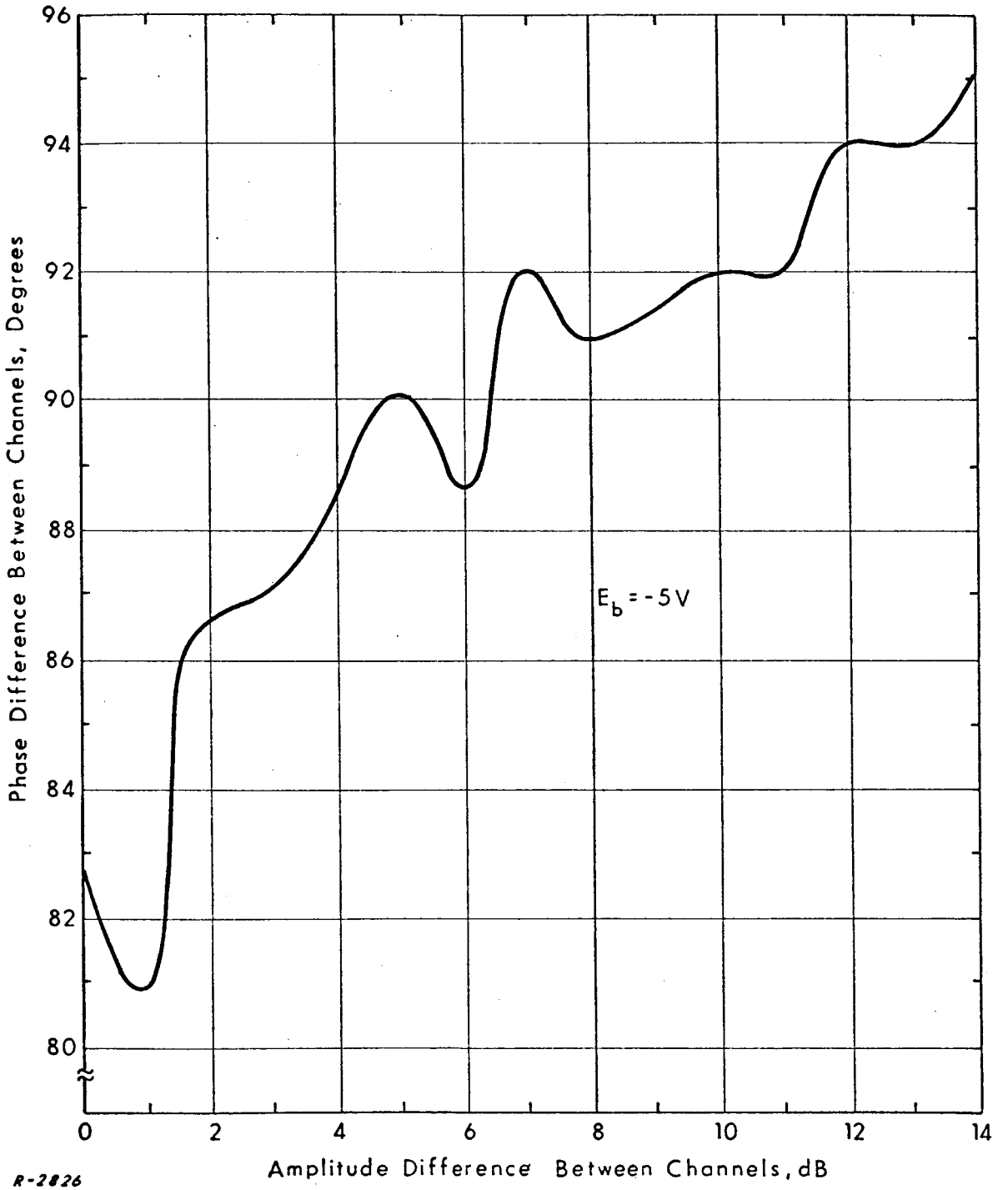


Fig. 3.6 Phase Difference Between Channels as a Function of Differential Input Signal Level.

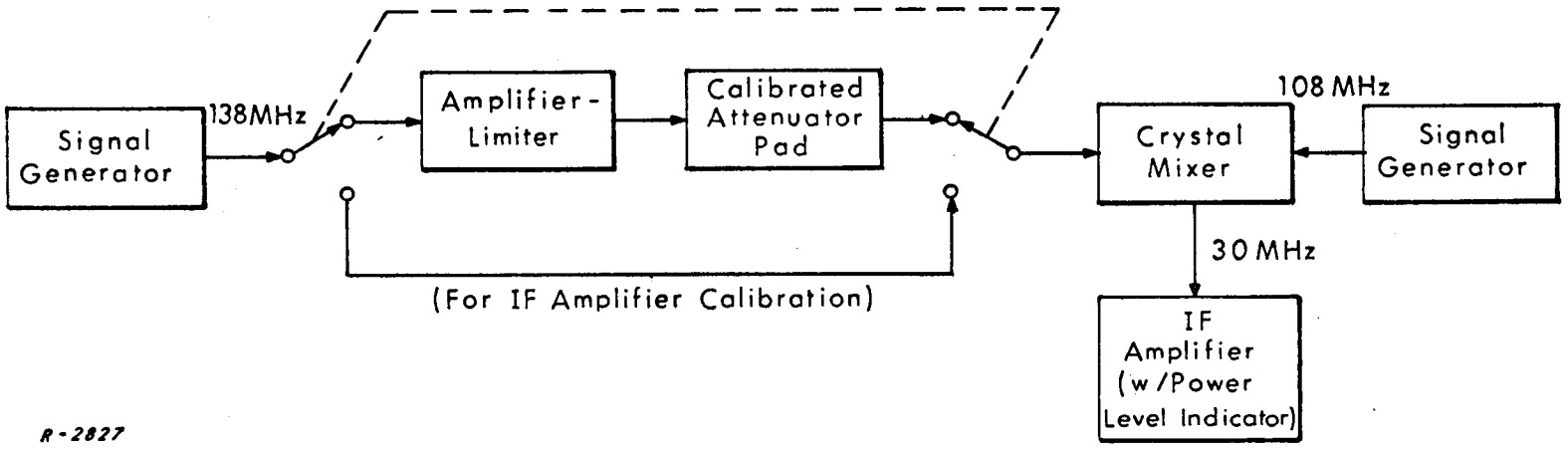


Fig. 3.7 Test Setup for Measurement of Amplifier-Limiter Amplitude Limiting Characteristics.

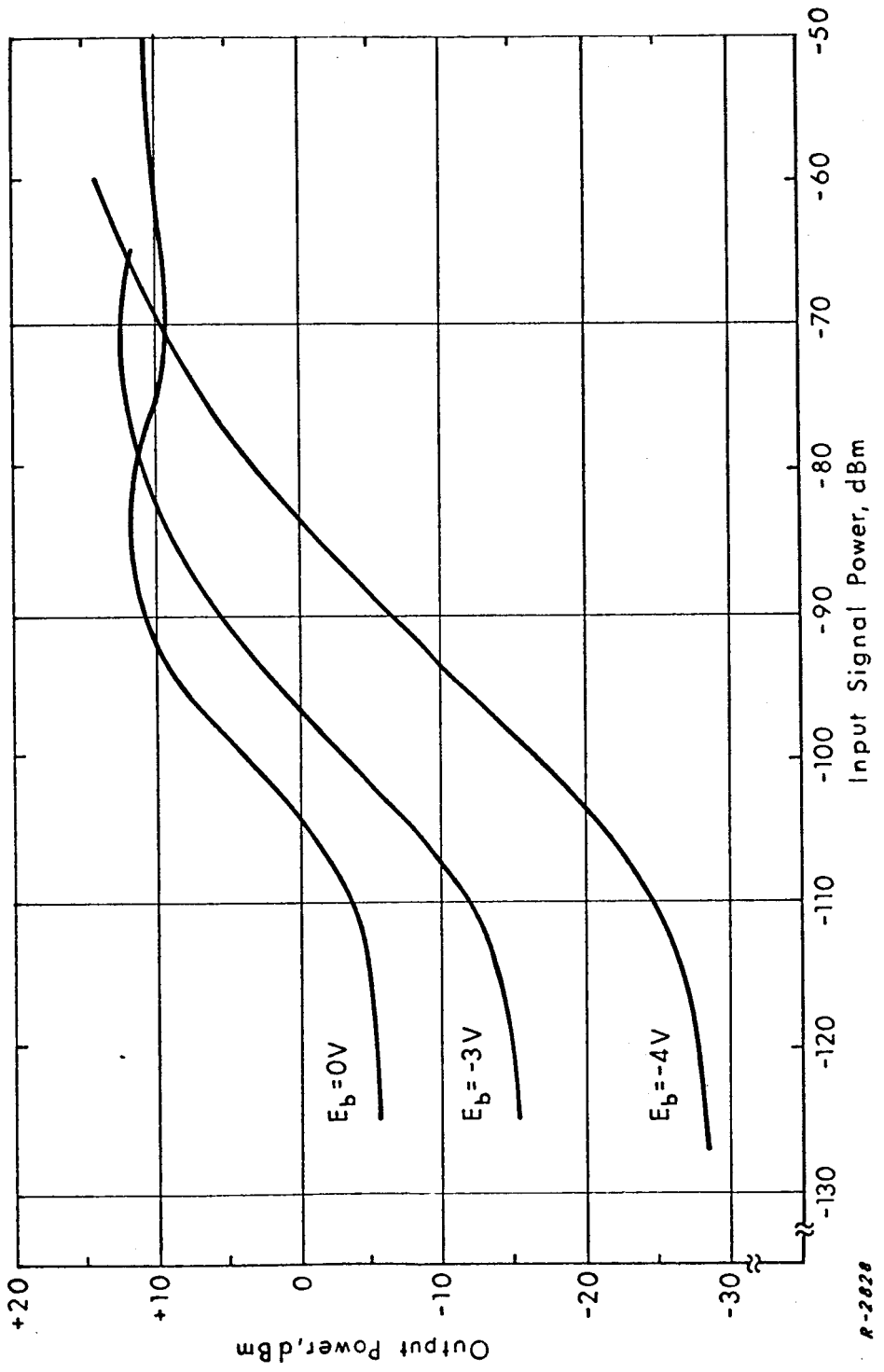


Fig. 3.8 Output Signal Power as a Function of Input Signal Power.

dynamics, virtually no limiting takes place when the bias setting is -4 volts. (This finding, incidentally, probably explains the reason maximum amplifier-limiter phase linearity occurs at a bias setting of -4 volts.)

### 3.3.3 Conclusions

In view of the long warmup time of the tube-type amplifier-limiters tested, and their relatively poor phase differential and limiting characteristics under conditions of changing input signal level, the LEL model IF 30-6049 amplifier-limiters are not suitable for the system use proposed.

## 3.4 Reactive Multicouplers

The use of reactive multicouplers (as opposed to resistive devices) has been suggested by Auburn University for the required D/F system signal processing. Reactive devices offer two distinct advantages over their resistive counterparts:

(a) The net power loss through reactive multicouplers is minimal. In resistive power dividers and summers a significant amount of real power is dissipated in the form of heat, thus resulting in a net transmission loss. The power loss consideration is important since, in the circuit proposed, any insertion loss has an appreciable effect on the overall system noise figure.

(b) Isolation between output legs of power dividers, and between input legs of power summers, is inherent in the reactive devices. Were resistive multicouplers to be used, active circuitry would be required to effect this isolation without further loss of power. Isolation between legs of the multicoupler is required in order to prevent feedback of a signal from one of the output ports of the multicoupler to one of the other output ports (and similarly, from one of the input ports of the multicoupler when used as a summer to another input port of the device). Such feedback would create a phase error in the composite signals of the legs, thereby introducing an overall system measurement error.

### 3.4.1 Examination of Multicoupler Circuitry

In spite of their seeming advantages, there are certain potential problems in using reactive multicouplers. In order to explore these areas, the physical makeup of the device is examined. The circuit diagram of a reactive multicoupler is shown in Fig. 3.9.

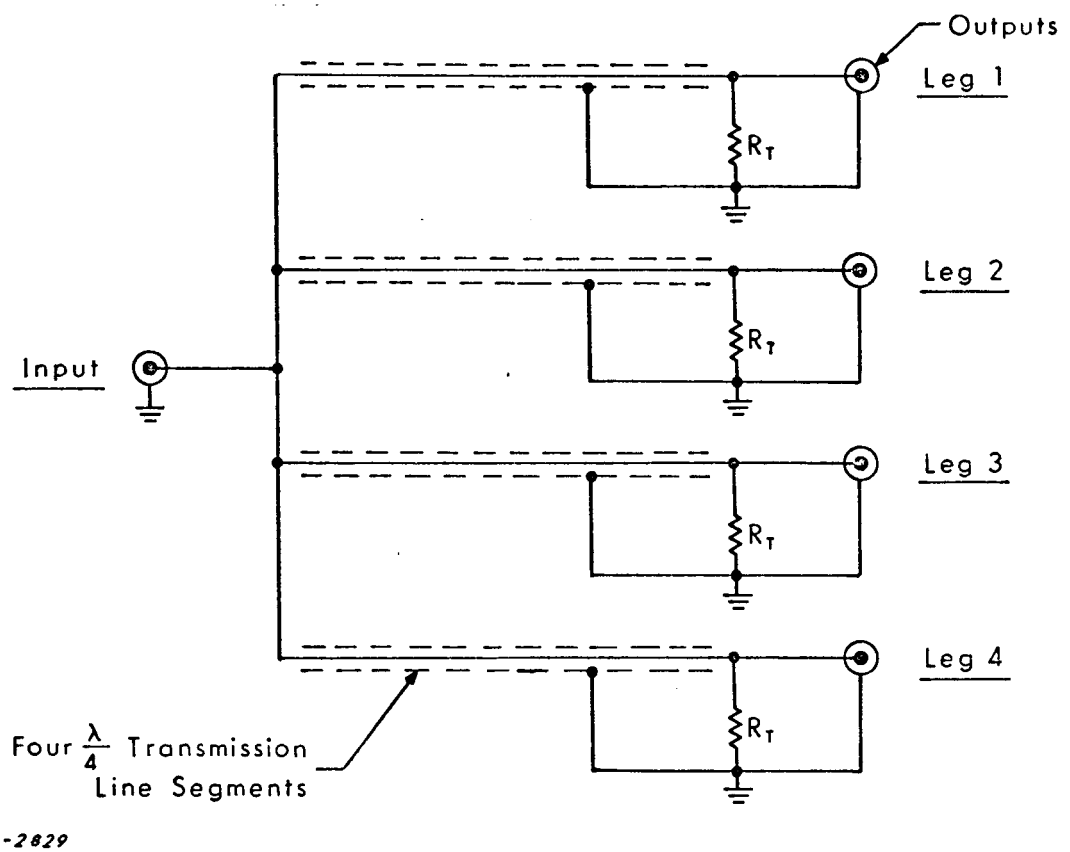


Fig. 3.9 Four-Port Reactive Multicoupler.

As is seen from the schematic, the device is comprised essentially of two types of circuit elements: resistors and $\lambda/4$ segments of coaxial transmission line. For input and output terminal impedances of 50 ohms, the characteristic impedance of the $\lambda/4$ segments of coaxial transmission line is 100 ohms. $R_T$ is 50 ohms.

The primary physical considerations relating to construction of reactive multicouplers are the following:

(1) Value of coaxial transmission line characteristic impedance.

(2) Length of coaxial transmission line segments.

(3) Resistance value of $R_T$.

If the above characteristic values do not fall within sufficiently accurate tolerances, significant errors may be introduced into the system by reactive multicouplers. Specifically, the errors which may be introduced include phase and amplitude errors in signal channels, and insufficient isolation between ports of the multicoupler. (Insufficient isolation would result in additional phase and amplitude errors in signal channels.)

### 3.4.2 Isolation Measurements

A reliable indicator of the acceptability of reactive multicouplers for use in the system proposed is the measurement of isolation between output ports of the divider (or input ports of the summer). Residual phase and amplitude errors originating in reactive multicouplers may be calibrated out by including the multicouplers in the network which includes the coaxial delay lines external to the multicouplers.

Isolation measurements were made on a typical four-port reactive (passive) multicoupler: LEL model MC 4-138. The following isolation readings were measured:

| Measurement Between Ports | Isolation in dB at 120 MHz | 138 MHz | 160 MHz |
|---|---|---|---|
| 1 and 2 | 25.6 | 37.3 | 24.4 |
| 1 and 3 | 24.0 | 34.4 | 26.6 |
| 1 and 4 | 24.8 | 34.8 | 25.0 |
| 2 and 3 | 25.1 | 37.8 | 24.9 |
| 2 and 4 | 24.1 | 32.8 | 26.2 |
| 3 and 4 | 25.2 | 39.0 | 25.2 |

Note that at the assumed carrier frequency the isolation between any two ports is at least 32.8 dB. Measured insertion loss was less than 0.5 dB over power division for each port.

### 3.4.3 Conclusions

Assuming little degradation in performance characteristics due to time or temperature, reactive multicouplers appear to be a satisfactory choice for the system use proposed.

# 4. ALTERNATE DIRECTION-FINDING RECEIVER DESIGNS

Some of the weaknesses in the original direction-finding receiver design were discussed in the previous chapter. In this chapter some alternate design approaches are considered which are intended to overcome the problem areas characteristic of the original system.

The following guidelines are adhered to in the development of alternate VHF direction-finding (D/F) receiver designs:

a. The D/F receiver must function over the operating dynamic range of the AROD Station Control Receiver.

b. Alternate designs must provide for direct substitution of the new D/F receiver in the presently conceived VHF antenna system.

c. The requirement for high reliability dictates minimum circuitry consistent with required performance; circuits employed must be within the current state-of-the-art.

d. Alternate D/F receiver designs must provide for sufficient stability to maintain antenna pointing position accuracy for long periods of time without the necessity for equipment adjustments or calibration.

## 4.1 Receiver Development

One of the most important considerations in the development of alternate D/F receiver designs for the AROD VHF antenna system is the dynamic range of input signals coupled to the receiver. With the establishment of the requirement that the receiver function adequately at very low input signal power, an inevitable question ensues as to whether an automatic tuning technique such as phase-lock should be employed in the receiver. In accordance with previously established guidelines, a dynamic range of -130 dBm to -60 dBm is required of the D/F receiver. Assuming the following parameters, the required noise bandwidth of the outputs to the phase meter is computed:

$S_{min}$ = Lowest Carrier Power Expected at Input to D/F Antenna = -130.0 dBm (4.1)

$N_o$ = System Input Noise Density (at $2000^oK$) = $-165.6 \frac{dBm}{Hz}$ (4.2)

$G_{ant}$ = Minimum D/F Antenna Gain (including a 6 dB margin allowance for antenna patterns of individual rings) = -8.0 dB (4.3)

T = D/F System Threshold, SNR = +8.0 dB (4.4)

The required noise bandwidth for satisfactory operation of the system is:

$$B_n = S_{min} - N_o + G_{ant} - T = -130.0 + 165.6 - 8.0 - 8.0 \quad (4.5)$$

$$= 19.6 \text{ dB greater than } 1 \text{ Hz} = 91.2 \text{ Hz} \approx 90 \text{ Hz} \quad (4.6)$$

Because of a maximum anticipated doppler shift of ±6 kHz and the noise bandwidth requirement of Eq. (4.6), the use of phase-locked techniques for removal of doppler from the carrier appears desirable.

### 4.1.1 Channel Requirements

Since there are two "rings" in the D/F antenna proposed by Auburn University, a total of six channels of information is produced: a reference channel for each ring, and $\underline{\ell}$ and $\underline{m}$ information channels for each ring. A design compromise is possible concerning the number of channels required in the D/F receiver. By time sharing one channel in each ring between $\underline{\ell}$ and $\underline{m}$ inputs (this feature was implemented in the original D/F receiver design), the total number of D/F receiver channels required may be reduced to four.

The use of four channels allows simultaneous monitoring of signal strength in both Z and XY rings to facilitate selection of the ring ultimately to be used for directional control of the S-band antenna. Assuming that the reference channel in each ring is, indeed, a valid criterion for selection of the ring whose signals will control the S-band antenna steering, the number of channels required in the D/F receiver may be further reduced to three.

A three-channel D/F receiver would require the time sharing of $\underline{\ell}$ and $\underline{m}$ signals from both Z and XY rings.

It is possible to reduce the number of channels required in the D/F receiver to two by employing all of the time-sharing techniques discussed above, plus the sequential sampling of Z and XY reference channels to determine the better ring for steering control of the S-band antenna. The use of this technique is questionable, however, because the signal quality samples thus obtained may not be as valid as continuously monitored information and usable phase measurements could be made during only a portion of the total sampling period.

At least two frequency conversions are desirable in the D/F receiver to provide adequate image rejection and avoid unnecessarily complex preselectors. Three frequency conversions may be necessary for translation of the signals to center frequencies suitable as inputs to some phase meters.

It is desirable to have the first frequency conversion in the D/F receiver occur after the attenuator and phase shifters used to normalize the four signal channel voltages in each ring, because the amount of phase shift required is easier physically to implement at the carrier frequency (138 MHz) than at some lower intermediate frequency.

### 4.1.2 Suggested Receiver Design

One receiver embodying the criteria discussed above is shown in Fig. 4.1*. The local oscillator signals $e_1$ and $e_2$ shown in this suggested design are developed in the Station Control Receiver, which has buffered outputs suitable for coupling to the VHF D/F receiver at the interfaces shown. Local oscillator signals $e_1$ and $e_2$ are nominally 96.3 MHz and 32.1 MHz, respectively. Through the use of a phase-locked carrier loop in the Station Control

* On all figures in this chapter, switches ($S_2$, $S_3$, etc.) are numbered to correspond with the D/F receiver designations of References 1 and 2.

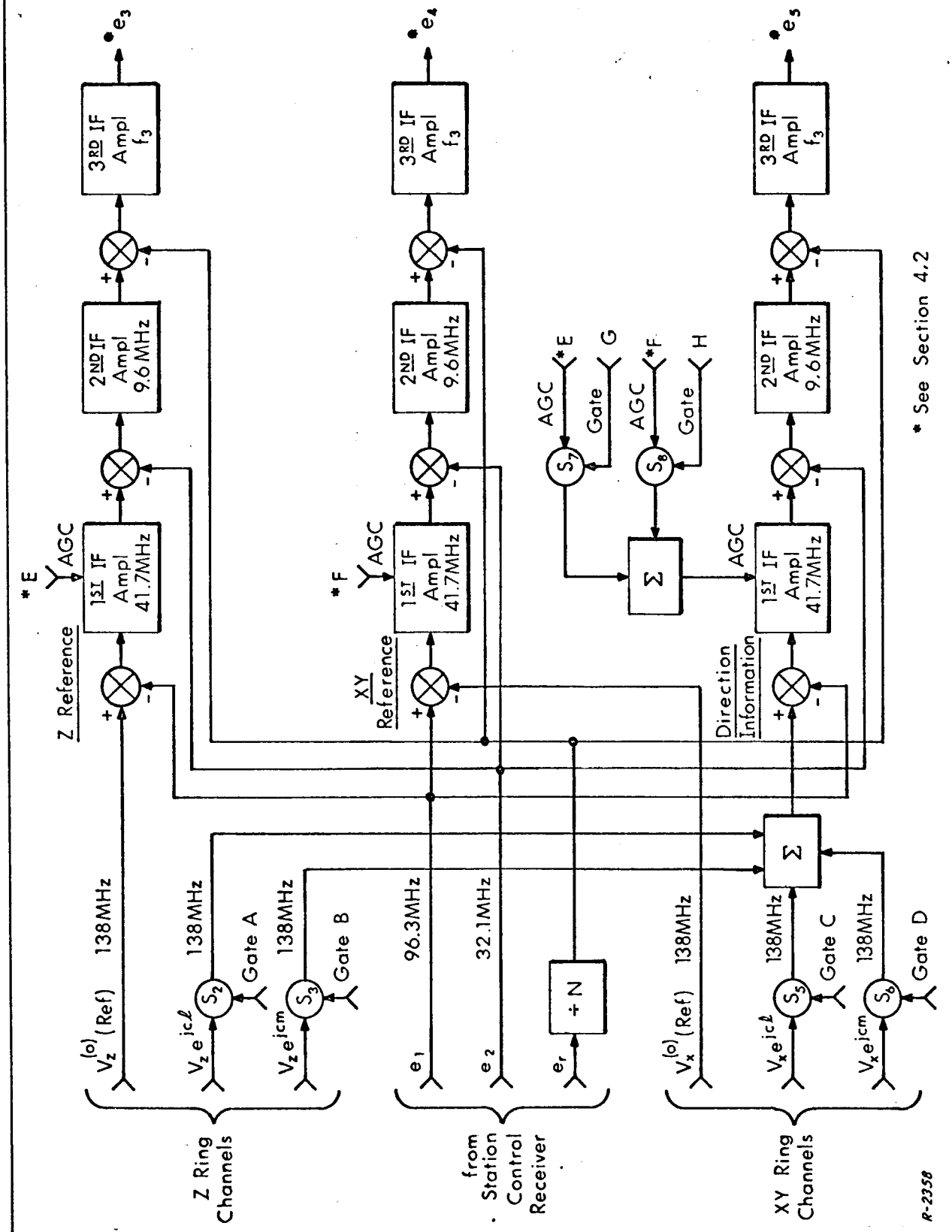


Fig. 4.1 VHF Direction-Finding Receiver.

Receiver, these local oscillator signals contain the proper frequency shifts for complete removal of doppler from the signal at the outputs of the second IF amplifier in the proposed D/F receiver.*

Conversion of second IF outputs to a third intermediate frequency is required for most phase measurement techniques. The stable local oscillator required for this conversion may be derived by frequency division/synthesis of the reference signal $e_r$ coupled from the Station Control Receiver. The constraints on the upper and lower bounds of the third IF design center frequency $f_3$ are the following: (1) the IF center frequency must be within the input frequency range of the phase meter, (2) if conventional noise filtering techniques are employed, the IF center frequency must be low enough to permit the use of filter circuits with practically realizable Q's, and (3) judicious choice of the IF center frequency must be made so that if foldover of modulation sidebands at zero frequency occurs, any resulting sideband products do not fall within the third IF passband.

Suitable local oscillator signals for all three stages of conversion could be developed within the D/F receiver by a scheme similar to that employed in the Station Control Receiver. Since these signals are conveniently available within the Station Control Receiver, however, it is reasonable to avoid duplication of circuitry by simply coupling them to the D/F receiver. The use in the D/F receiver of the local oscillator signals developed in the Station Control Receiver requires the intermediate frequencies shown in Fig. 4.1. If, for some reason, other intermediate frequencies are desired, it would then be necessary to generate the proper signals within the D/F receiver.

Use of AGC is indicated due to the large dynamic range of input signals to the D/F receiver. AGC feedback to the first intermediate frequency amplifier – and RF amplifiers, if required – permits operation of the relatively

* See Appendix A.

narrowband second intermediate frequency amplifiers at constant gain. This technique enhances the phase characteristics of the receiver as a function of signal dynamics by gain control of comparatively wideband stages.

Switching of direction information signals $V_z e^{jc\ell}$, $V_z e^{jcm}$, $V_x e^{jc\ell}$, and $V_x e^{jcm}$ to the D/F receiver direction information channel is accomplished by gating signals and switches. The switching operation is sequential and periodic for $\ell$ and m information signals, and depends on which ring – Z or XY – provides the more reliable information for S-band antenna switching.

The development of AGC voltages and their switching, as well as signal selection criteria and the development of appropriate gating signals, will be covered in a forthcoming Technical Report.

The long-term phase stability characteristics of the individual channels in the D/F receiver proposed are of particular importance. Amplifier/filter phase drift must be minimized in the design suggested, since the characteristics of reference and directional information channels are independent of one another. Temperature compensation of the various stages would undoubtedly be necessary for the required stability.

4.1.3 Alternate Suggested Design

Another approach worthy of consideration in view of the critical channel phase differential stability requirements outlined in the previous paragraph is the one shown in Fig. 4.2. The signal inputs are switched in the same manner as in Fig. 4.1. Local oscillator signal $e_1$, however, is supplemented in the alternate design by local oscillator signals $e_6$ and $e_7$. As a result the Z and XY reference signals are offset in frequency at the input to the first IF amplifier by ±300 kHz, respectively, thus allowing the use of a single receiver channel for the amplification and conversion of all three signals. More important than the possible value of elimination of two entire channels of equipment,

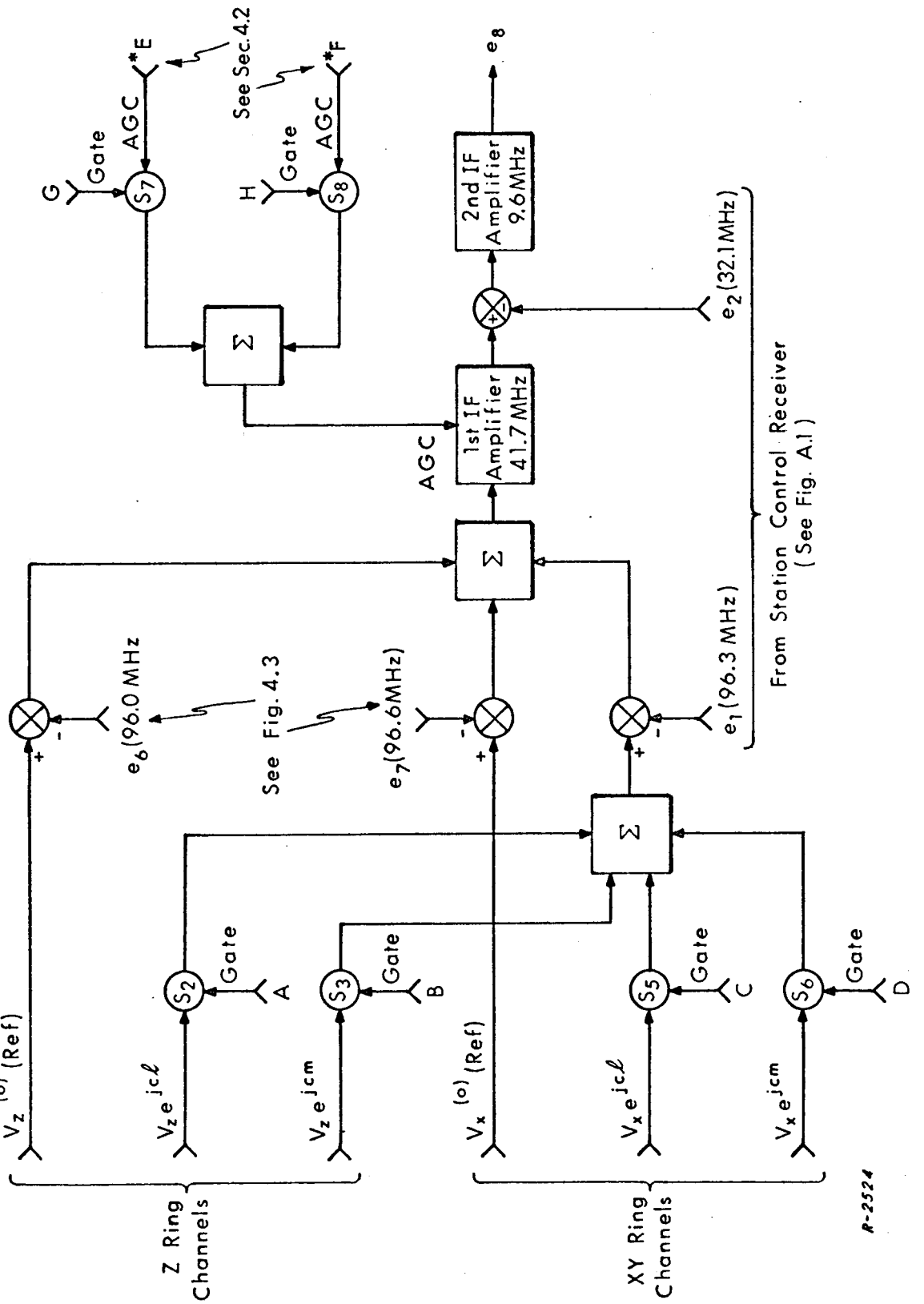


Fig. 4.2 Alternate Design VHF Direction-Finding Receiver.

is the fact that the problem of differential phase stability is reduced to a minimum by passing all three signals through a common channel.

The bias frequency offset introduced to the two reference signals through the synthesis of local oscillator signals $e_6$ and $e_7$ is a constant. Although the center frequencies of the three signal components coupled to the second IF amplifier are staggered, complete removal of doppler from all signals is effected by utilization of local oscillator signal $e_1$ in the synthesis of $e_6$ and $e_7$.

Examples of the synthesis of signals $e_6$ and $e_7$ for the receiver design depicted in Fig. 4.2 are shown in Figs. 4.3a and 4.3b. Figure 4.3a shows a synthesizer which uses conventional filters. Care must be taken in the design and construction of filters, if this technique is used, so that the phase of the reference signal carriers is not altered as a function of temperature and doppler frequency changes. $e_9$ and $e_{10}$ are synthesized by mixing $e_r$ and frequencies derived from $e'_r$. $e_r$, $e_9$, and $e_{10}$ are used as third local oscillator signals (see Fig. 4.7).

Phase-locked loops may also be used as filters in the synthesis of local oscillator signals $e_6$ and $e_7$, as shown in Fig. 4.3b. Among other factors, the frequency dynamics of $e_1$ as contributes to the loop phase error must be considered, since this error affects the directional steering accuracy of the overall antenna system.

## 4.2 Noise Bandwidth Considerations

Several methods are possible for achieving the 90 Hz noise bandwidth required of the D/F receiver. Two types of filtering techniques are discussed below, one involving the use of phase-locked loops (PLL's), and the other utilizing conventional filters.

### 4.2.1 Phase-Locked Loop as a Filter

By employing the phase-locked loop as a filter, the noise bandwidth requirement of Eq. (4.6) may readily be achieved. In the method depicted in

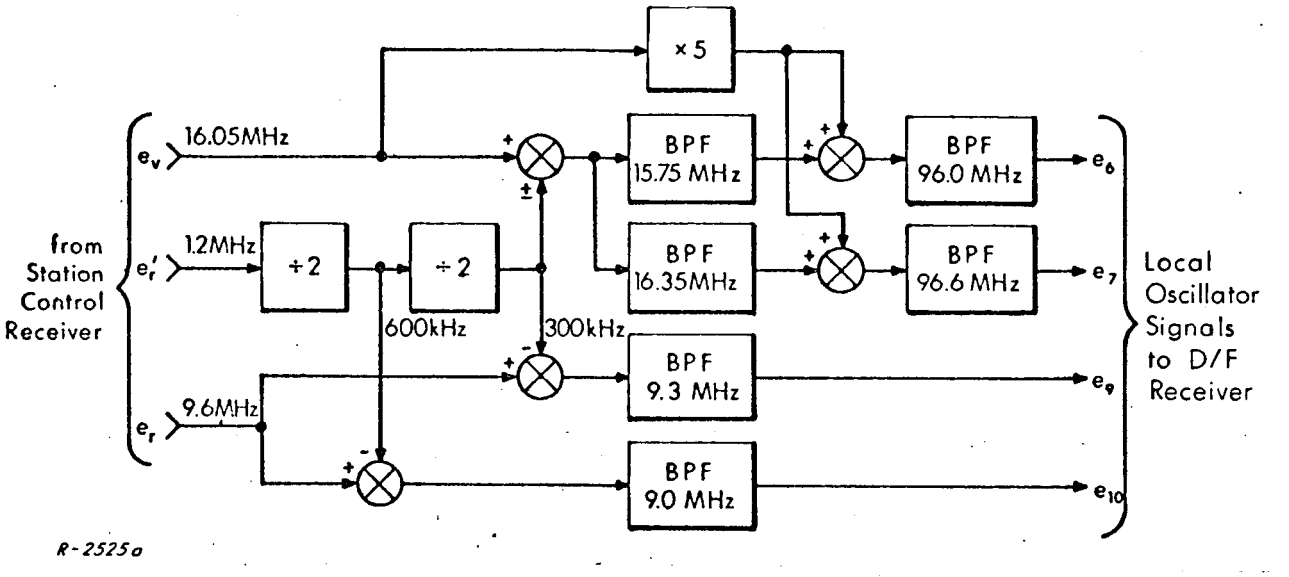


Fig. 4.3a Frequency Synthesizer Using Conventional Filtering.

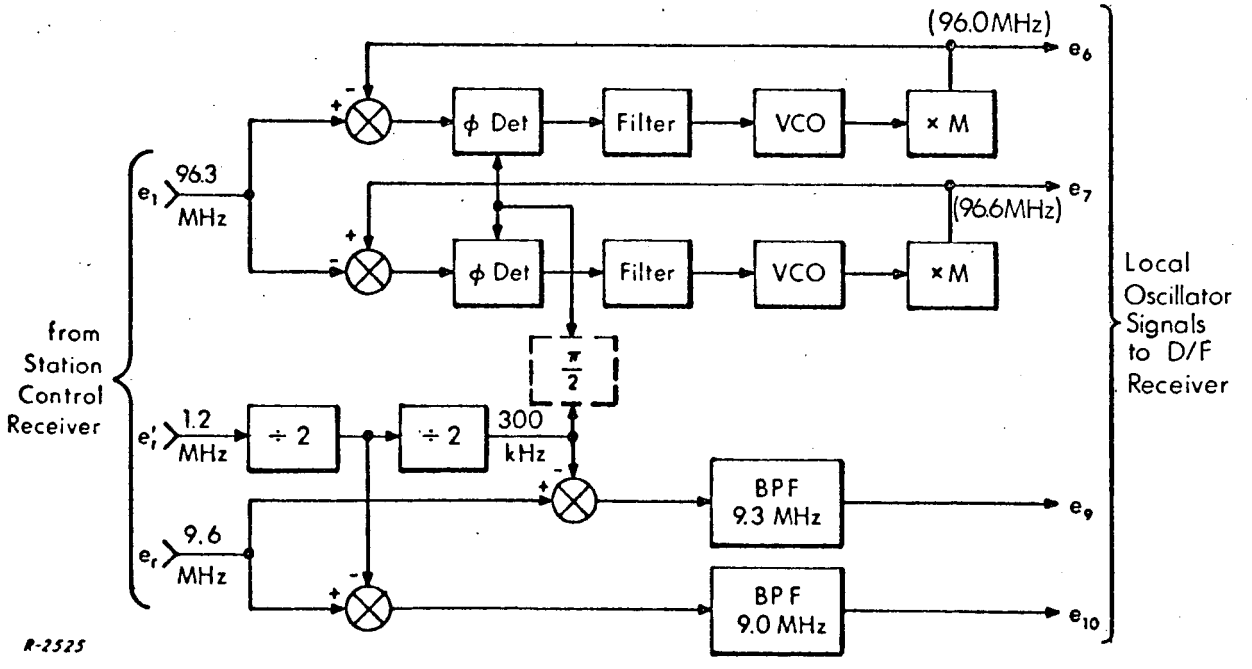


Fig. 4.3b Frequency Synthesizer Using Phase-Locked Filtering.

Fig. 4.4, outputs from the third IF amplifier in the D/F receiver of Fig. 4.1 are coupled to the PLL's. The net effect of utilizing the carrier tracking loop in the Station Control Receiver to provide the first and second local oscillator signals for the D/F receiver is that there are no carrier frequency dynamics for the filtering PLL's to track out. This technique allows the loops to operate at noise bandwidths much less than 90 Hz to reduce the noise on the signals coupled to the phase meter. In addition, the narrower bandwidths might allow RF amplifiers to be eliminated from the system with a consequent increase in system noise figure. The advantages of elimination of RF preamplifiers are the following: (1) the problem of obtaining the required differential phase stability between channels is greatly reduced if no RF preamplifiers are required and the receiver design shown in Fig. 4.2 is implemented, and (2) standby primary power requirements are greatly reduced.

Prior to PLL acquisition, any frequency difference between the output signal of the third IF amplifiers ($e_3$, $e_4$, or $e_5$) and the rest frequency of the corresponding loop VCO, will be caused primarily by drift in the VCO. Assuming a worst-case frequency instability of five parts in $10^5$ in a passively temperature compensated 100 kHz VCO, the frequency uncertainty in the loop is 5 Hz. The acquisition time may be approximated for a critically damped loop ($\zeta = \frac{1}{\sqrt{2}}$) as follows:

$$t_f \approx \frac{33.5\,(\Delta f)^2}{B_n^3} \tag{4.7}$$

where

$t_f$ = approximate frequency lock time, seconds,

$\Delta f$ = frequency uncertainty, Hz, and

$B_n$ = two-sided noise bandwidth, Hz.

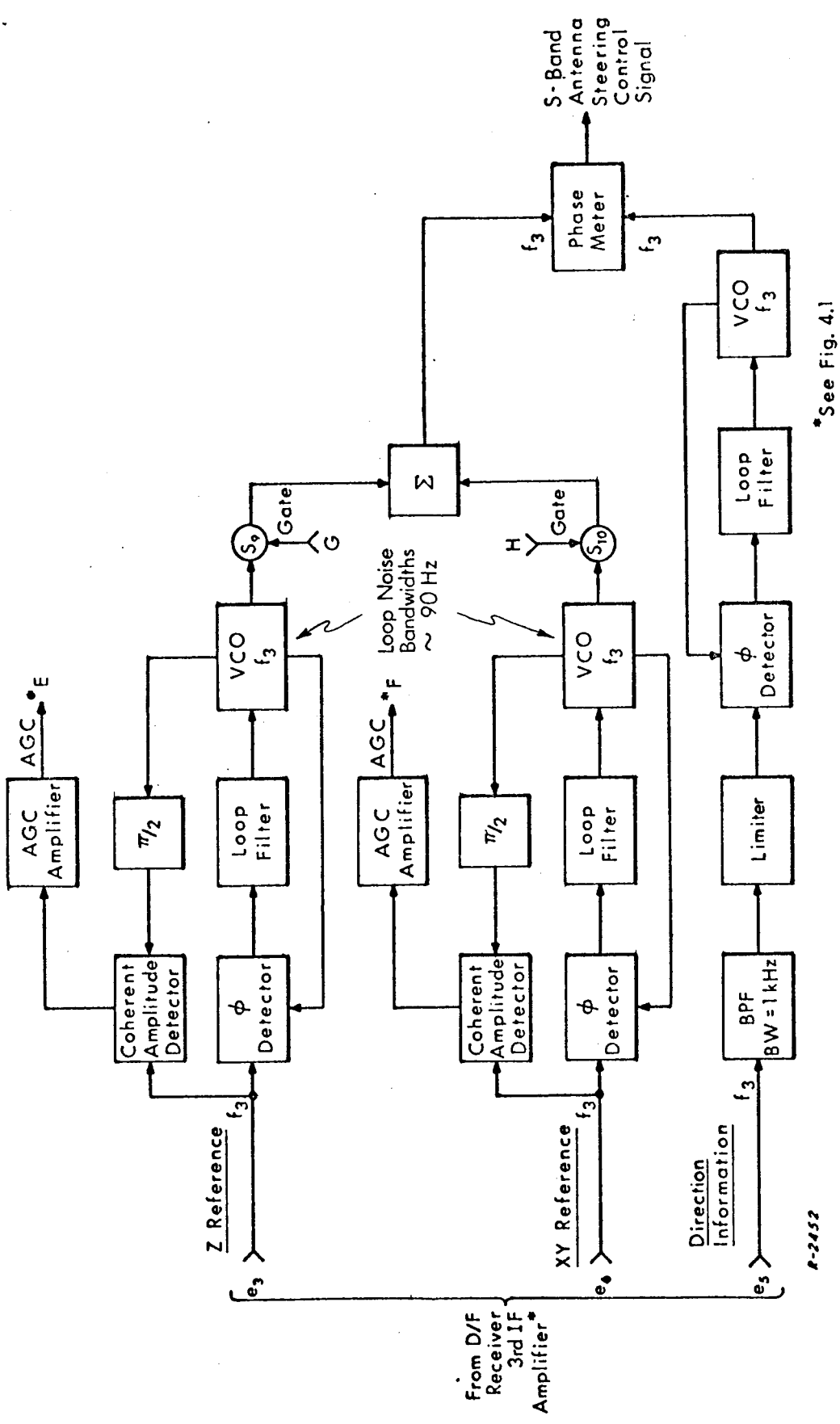


Fig. 4.4 PLL Filtering for 3-Channel D/F Receiver.

Thus, for a 90 Hz noise bandwidth:

$$t_f \approx 1.1 \text{ milliseconds} \tag{4.8}$$

For a 30 Hz noise bandwidth:

$$t_f \approx 31 \text{ milliseconds} \tag{4.9}$$

In addition to the time required for frequency acquisition of the PLL, the time for phase transient errors to subside must be considered. Normalization of experimental data obtained by ADCOM* indicates the phase acquisition time $t_\phi$ for this loop to be on the order of 0.3 milliseconds.

The total lock time $t_L$ is:

$$t_L = t_f + t_\phi \tag{4.10}$$

which may be approximated to:

$$t_L \approx t_f \tag{4.11}$$

for $t_f >> t_\phi$. Thus, $t_L \approx 1.4$ milliseconds for a loop with $B_n = 90$ Hz.

Of considerably more importance than the ability of PLL's to track any slowly changing frequency dynamics in the input signal is their ability to reacquire each time the input signal changes. Since $\underline{\ell}$ and $\underline{m}$ signals are periodically time shared in the D/F receiver direction information channel, the PLL in that channel must reacquire each time the input signal is switched from $\underline{\ell}$ to $\underline{m}$ information and again when the signal changes back from $\underline{m}$ to $\underline{\ell}$ information. The loop must also reacquire each time steering information is selected from a different ring. If the switchover of input signals is instantaneous, the VCO will not return to its rest frequency, but will remain at the frequency common to the two input signals. Thus, $t_L$ will be equal to $t_\phi$. Acquisition time ($t_L$) of the

* Boardman, C.J. and Filippi, C.A., "Sawtooth PLL Acquisition Experiments," ADCOM Report No. 566-RR-49, 1965.

loop under this condition will probably be less than one millisecond, since the input signal switchover time can be made to be virtually instantaneous. The loop acquisition times calculated are small compared to $\underline{\ell}$ and $\underline{m}$ sequence and information sampling periods.

Coherent AGC systems are convenient byproducts of the use of PLL's as shown in Fig. 4.4. Whenever the selection of direction information is changed from Z to XY rings, or vice-versa, there will be a period concurrent with PLL reacquisition during which IF amplifier gain transients will occur due to the switching of AGC and input signals. Since such switching times are virtually instantaneous and the IF amplifier is relatively wideband, any resulting gain transient period would probably be negligible.

The AGC input controlling the gain of the Direction Information channel first IF amplifier* is switched between AGC voltages E and F from the two reference channels.** $e_3$ and $e_4$ are thus held constant by AGC systems in their respective channels. $e_5$, however, will vary in amplitude as a function of the direction from which the transmitting source is radiating. Since the noise bandwidth of the PLL in the direction information channel would also vary as a function of this input signal level, a narrowband limiter is employed prior to the PLL to normalize the input signal amplitude, and thus hold the noise bandwidth fairly constant. The bandpass filter in front of the limiter will keep the signal-to-noise ratio at the input to the limiter within acceptable limits. A 1 kHz bandwidth filter will provide an approximate -2 dB minimum SNR at the Direction Information channel PLL input.

---

* See Fig. 4.1.

** Operation of direction information and reference channels at equal gain is desirable to eliminate phase differentials between the two channels which might occur if separate AGC sources, and therefore separate IF amplifier gains, were employed. See Fig. 4.4 for derivation of AGC voltages.

Gating signals G and H switch the reference signal from either the Z ring channel or the XY ring channel to the phase meter, where the phase of the appropriate direction information signal with respect to the reference is measured for directional control of the S-band antenna. Development of these gating signals, as well as phase metering techniques, will be discussed in a forthcoming Technical Report.

Three phase-locked loops may be used to filter the frequency-staggered carriers of the receiver design of Fig. 4.2 in the manner shown in Fig. 4.5. Each of the loops is phase-locked to a different carrier component coupled from the second IF amplifier. The outputs of the loops are then translated to a common center frequency (300 kHz in the example) by mixing them with $e_r$, $e_9$, and $e_{10}$, the latter two being local oscillator signals derived from the Station Control Receiver reference oscillator (see Figs. 4.3a and 4.3b). Limiting in the direction information channel, development of AGC signals, and reference channel switching are as in Fig. 4.4.

### 4.2.2 Conventional Filters

Conventional filtering techniques may also be used to achieve the desired noise bandwidth. Figure 4.6 illustrates the method by which this may be accomplished. Outputs $e_3$, $e_4$, and $e_5$* are coupled from the third IF amplifiers of Z ring reference, XY ring reference, and direction information channels, respectively, to the bandpass filters. The 90 Hz noise bandwidth requirement of Eq. (4.6) necessitates that $f_3$ be a relatively low frequency in order that $\frac{f_3}{90}$ fall within the range of Q's possible in practical conventional filters. Noncoherent AGC detection is provided following the filters as shown in the figure.

The use of conventional filters for filtering of the carriers resulting from the circuit of Fig. 4.2 is shown in Fig. 4.7. Adjustment of the frequency of synthesized signals $e_9$ and $e_{10}$, and of the frequency scaling factors of $e_v$ and $e'_r$ (see Figs. 4.3a and 4.3b), is necessary in order to achieve the three 150 kHz

* See Fig. 4.1.

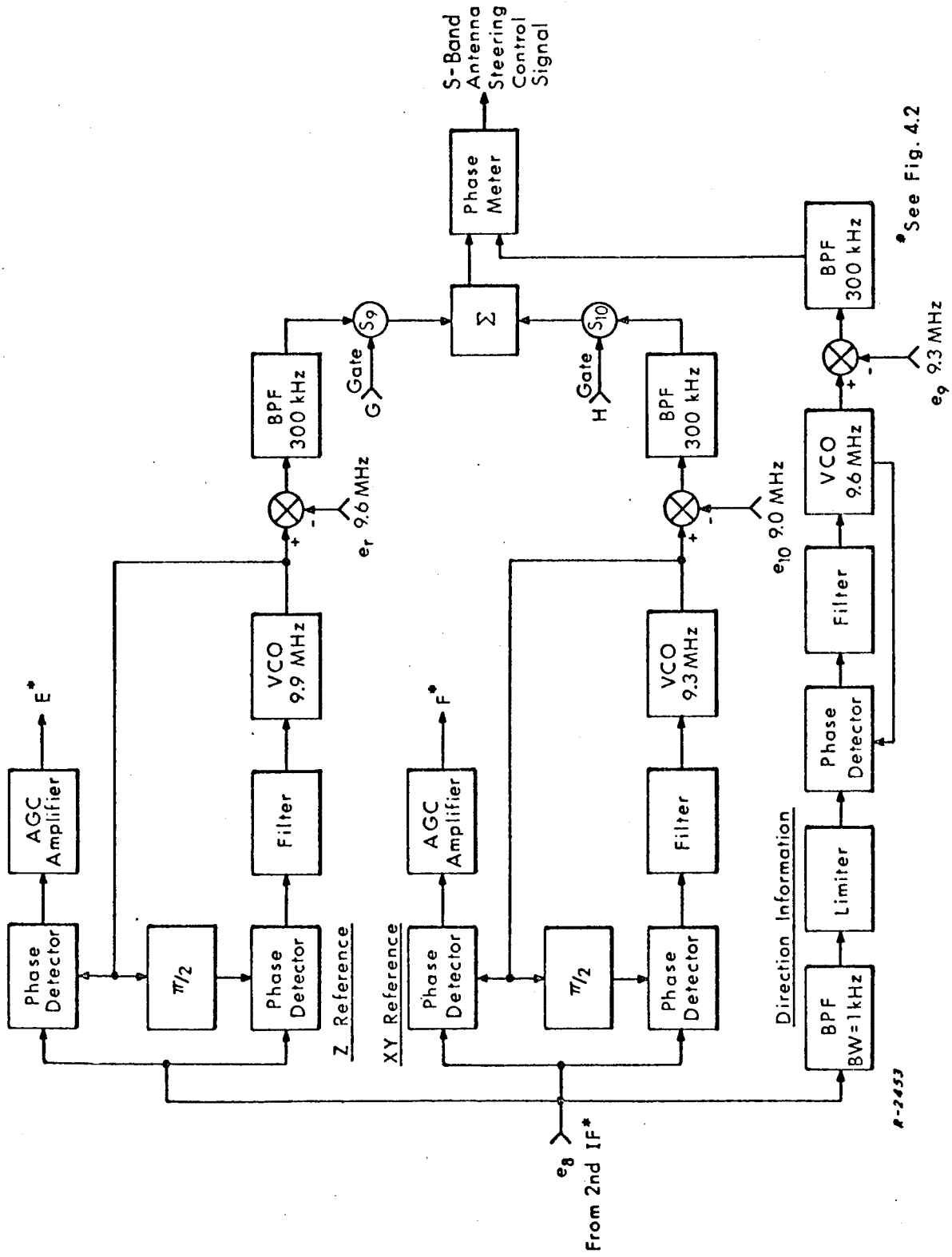


Fig. 4.5 PLL Filtering for Alternate Design D/F Receiver.

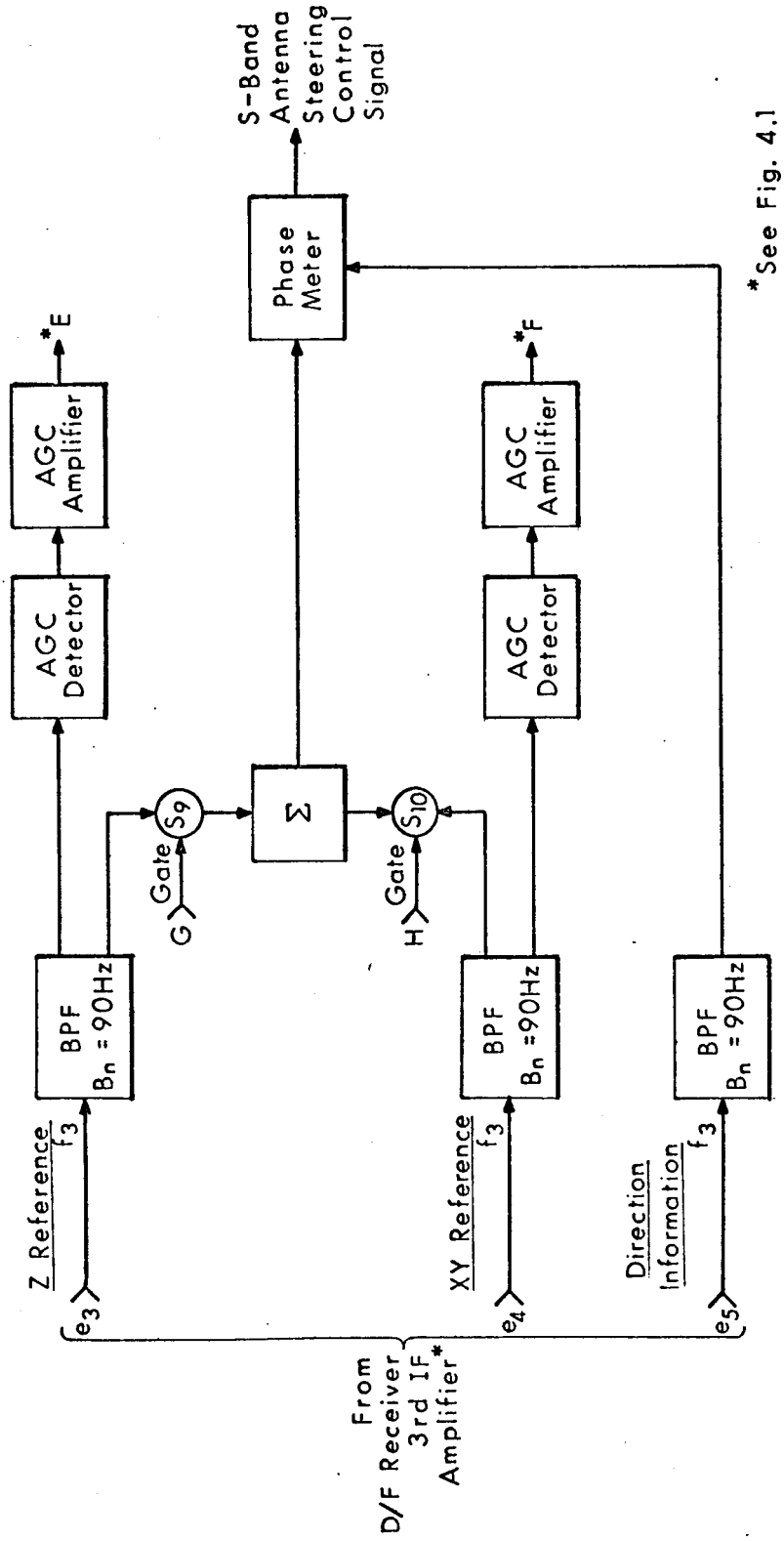


Fig. 4.6 Conventional Filtering for 3-Channel D/F Receiver.

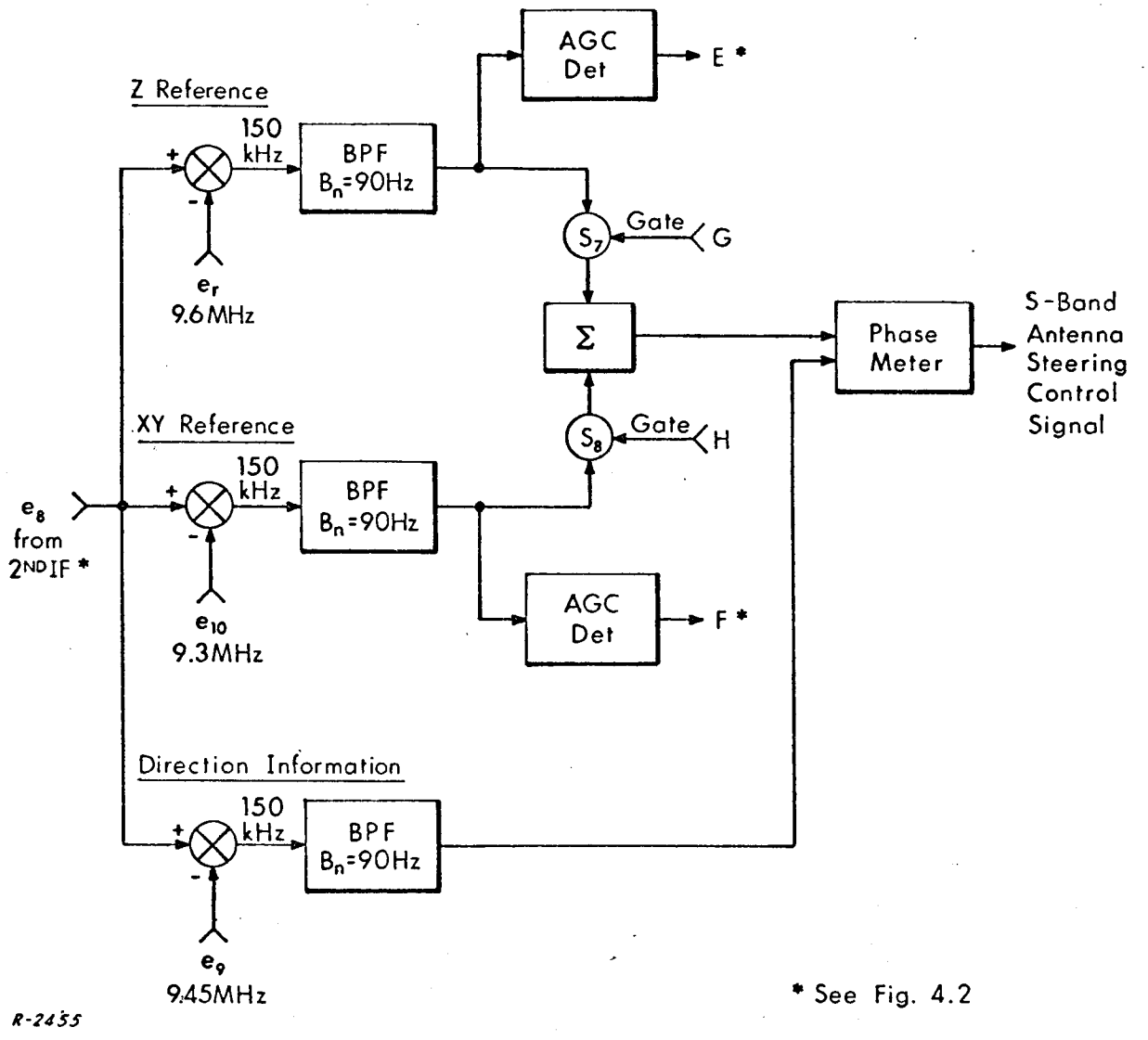


Fig. 4.7 Conventional BP Filtering for Alternate Design D/F Receiver.

carriers at the inputs to the bandpass filters. The constraint on the upper bound of this input carrier frequency is that it must be sufficiently low to accommodate the use of filters with practically realizable Q's. Assuming utilization of the conventional filter method of local oscillator synthesis,* the lower bound is dependent on the frequency separation possible between $e_r$ and $e_6$, and between $e_r$ and $e_7$, without phase distortion of $e_6$ and $e_7$ due to changes in doppler.

Four types of conventional filters are surveyed briefly below for the purpose of possible use in the circuits of Figs. 4.6 and 4.7:

a. Passive LC Filter: Q's of up to 20-30 are possible, meaning an upper bound carrier frequency $f_3$ of approximately 2.7 kHz would be required for use in the circuit of Fig. 4.6. Passive temperature compensation would be required for the desired phase and frequency stability. Passive filters could not be used in the circuit of Fig. 4.7 because of the high-Q filter requirement.

b. Active RC Filters: Q's of up to 50-100 are possible, meaning an upper bound carrier frequency $f_3$ of approximately 9 kHz would be required for use in the circuit of Fig. 4.6. Passive temperature compensation would probably be required for the desired phase and frequency stability. Active RC filters could not be used in the circuit of Fig. 4.7 because of the high-Q filter requirement.

c. Mechanical Filters: Q's of up to 10-1000 are possible. Center frequency may be held to within 2 parts per million per degree C over a range of -25°C to +85°C, meaning a ±17 Hz center frequency shift may occur in a filter with 75 kHz center frequency over the temperature range. Although no phase stability specifications are available for mechanical filters, available frequency stability specifications suggest that active temperature compensation might be required for the desired phase stability. The use of mechanical filters is marginal for the circuit of Fig. 4.7, but if the carrier frequency could be reduced to 75 kHz, they could be used.

---

* See Fig. 4.3a.

d. Crystal Filters: Q's of up to 120-2000 are commercially available. A 90 Hz noise bandwidth means a center frequency as high as 180 kHz could be used. Active temperature compensation would be required if needed for the desired phase and frequency stability. Crystal filters could be used in either the circuit of Fig. 4.6 or 4.7.

## 5. REFERENCES

1. Technical Report No. 5, "A VHF Direction Finding System," prepared by Auburn University Antenna Research Laboratory under NASA Contract NAS8-11251, E. R. Graf, Project Leader, January 19, 1966.

2. Final Report, "Automatically Scanned Antenna Systems," prepared by Auburn University Antenna Research Laboratory under NASA Contract NAS8-11251, E. R. Graf, Project Leader, January 20, 1966.

# APPENDIX A

## ANALYSIS OF DOPPLER FREQUENCY SHIFT ON LOCAL OSCILLATOR SIGNALS OF STATION CONTROL RECEIVER

The block diagram of the Station Control Receiver is shown in Fig. A. 1. The doppler frequency components of voltages $e_1$ and $e_2$ are computed below as a function of doppler frequency shift on the station control signal.

Writing the loop frequency equations for the Station Control Receiver

$$f_c - 3f_2 - f_2 = 9.6 \text{ MHz} \tag{A.1}$$

$$f_2 = 0.25\, f_c - 2.4 \text{ MHz} \tag{A.2}$$

Since $f_1 = 3f_2$,

$$f_1 = 0.75\, f_c - 7.2 \text{ MHz} \tag{A.3}$$

From Eqs. (A. 2) and (A. 3) it can be seen that

$$\delta_2 = 0.25\, \delta_c \tag{A.4}$$

and

$$\delta_1 = 0.75\, \delta_c \tag{A.5}$$

where $\delta_c$, $\delta_2$ and $\delta_1$ are doppler frequency shifts on $f_c$, $f_2$ and $f_1$ respectively. Under the conditions that $\delta_c = \pm 6$ kHz,

$$\delta_2 = \pm 1.5 \text{ kHz} \tag{A.6}$$

and

$$\delta_1 = \pm 4.5 \text{ kHz} \tag{A.7}$$

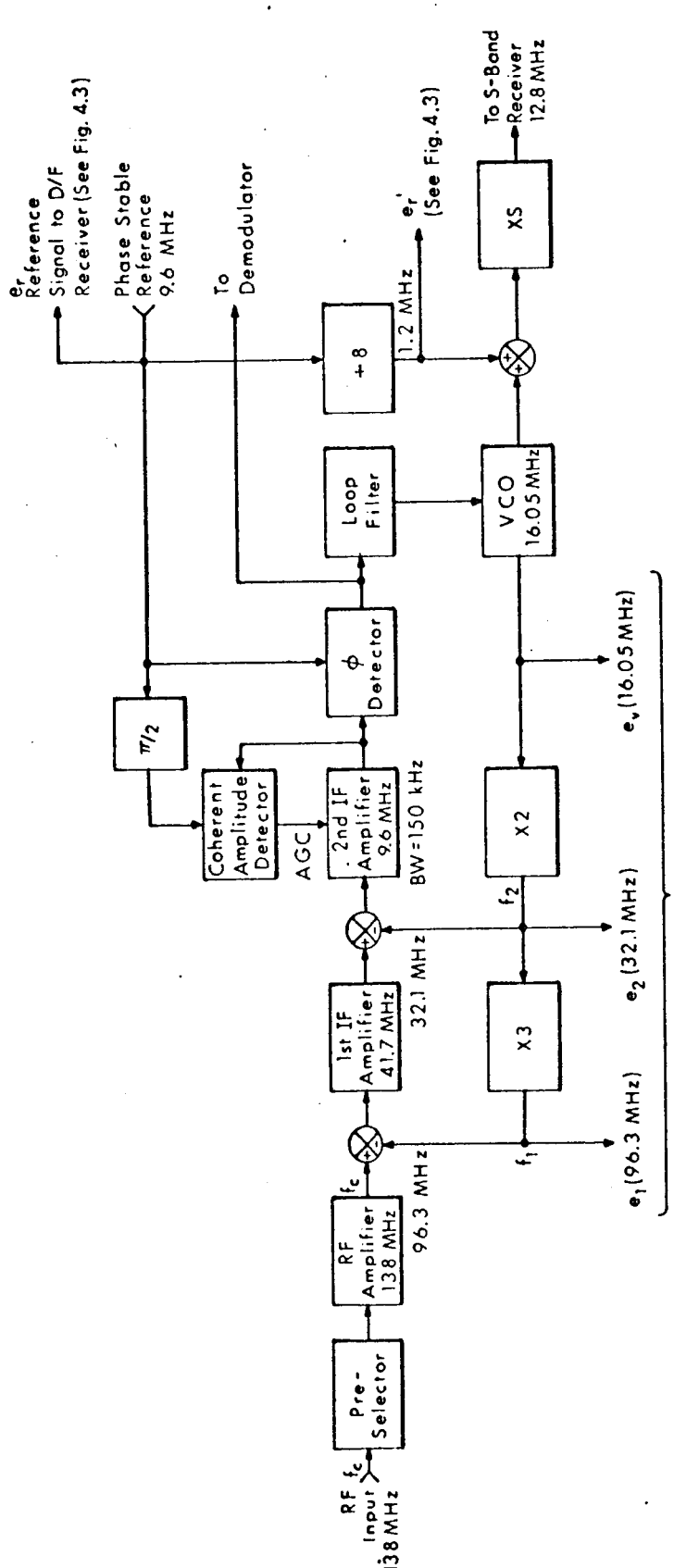


Fig. A.1 Station Control Receiver.

# APPENDIX B

## PHASE METER OUTPUT FILTERING

Lowpass filtering is required at the output of the phase meter to reduce the noise coupled to the A/D converter. Sequential sampling of $\underline{\ell}$ and $\underline{m}$ information results in a different dc level at the output of the phase meter during the period of $\underline{\ell}$ information sampling than for the period of $\underline{m}$. A single filter section such as that shown in Fig. B.1 could be employed to provide the necessary filtering, but since two output signals are alternately present, an error would exist until the capacitor in the filter charged to the analog value of the new signal.

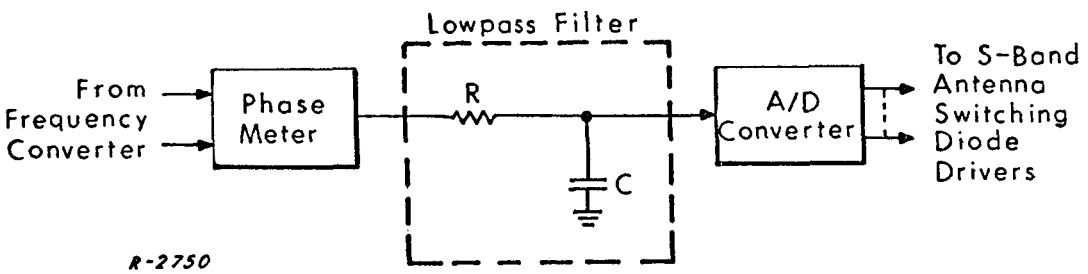


Fig. B.1 Phase Meter Output Coupled to Single Section Lowpass Filter.

The presence of such an error each time the input signal is switched would require a filter with a very short time constant in order that the total error be kept within acceptable limits.

A better approach for accomplishing the necessary filtering is the one shown in Fig. B. 2.

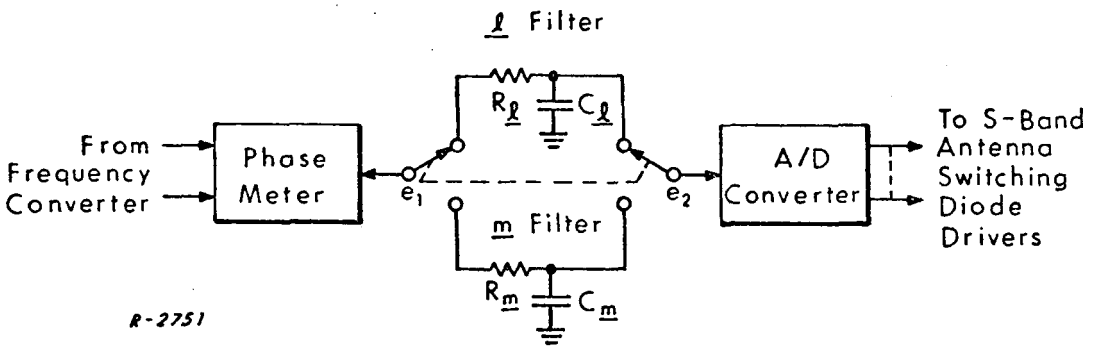


Fig. B. 2 Phase Meter Output Switched Between Two Lowpass Filters.

The inputs and outputs of two separate filters are switched synchronously with the sampling periods of ℓ and m information. During the period of ℓ information sampling, the ℓ filter capacitor charges to the dc level representing ℓ information. When the input signal is switched to m information, the m filter capacitor charges to the dc level representing m information. During the m filter charge period, the input and output of the ℓ filter are disconnected, and since there is no load on the ℓ capacitor, ℓ information is stored in the ℓ filter during the charge period of the m filter. Similar storage of m information occurs during the period of ℓ filter capacitor charge.

A switching period of one second for ℓ and m information sampling has been suggested. Such a period would result in ℓ and m filter integration times of 0. 5 second each, assuming alternate sampling. Information storage occurs during the half-period the alternate filter is integrating.

The upper bound of the filter time constant is determined by the amount of error to be tolerated due to filter capacitor charge lag. In the period immediately following signal acquisition this charge lag is potentially greatest. After the transient error caused by the acquisition process has subsided, only two sources of error remain: (1) error due to filter capacitor leakage, either internal or through the A/D converter load, and (2) error due to vehicle flight dynamics. The error due to capacitor leakage may be made negligible by proper selection of the type* and value of the filter capacitor. The error due to vehicle dynamics is a consideration solely of the filter time constant, assuming an ideal system. This time constant should be sufficiently short that when the rates of change of $c\ell$ and cm are maximum, the error is within tolerable limits. This condition will be satisfied if the time constant is chosen to result in an acceptable acquisition transient error with a maximum initial $c\ell$ or cm offset.

The filter time constant lower bound is determined by the error to be tolerated due to noise. The time constant chosen to satisfy the error requirement imposed by the filter capacitor charge lag will easily fulfill the lower bound time constant constraint.

B.1 Maximum Rates of Change of $c\ell$ and cm

The near-earth orbital path of the vehicle is shown in the diagram of Fig. B.3.

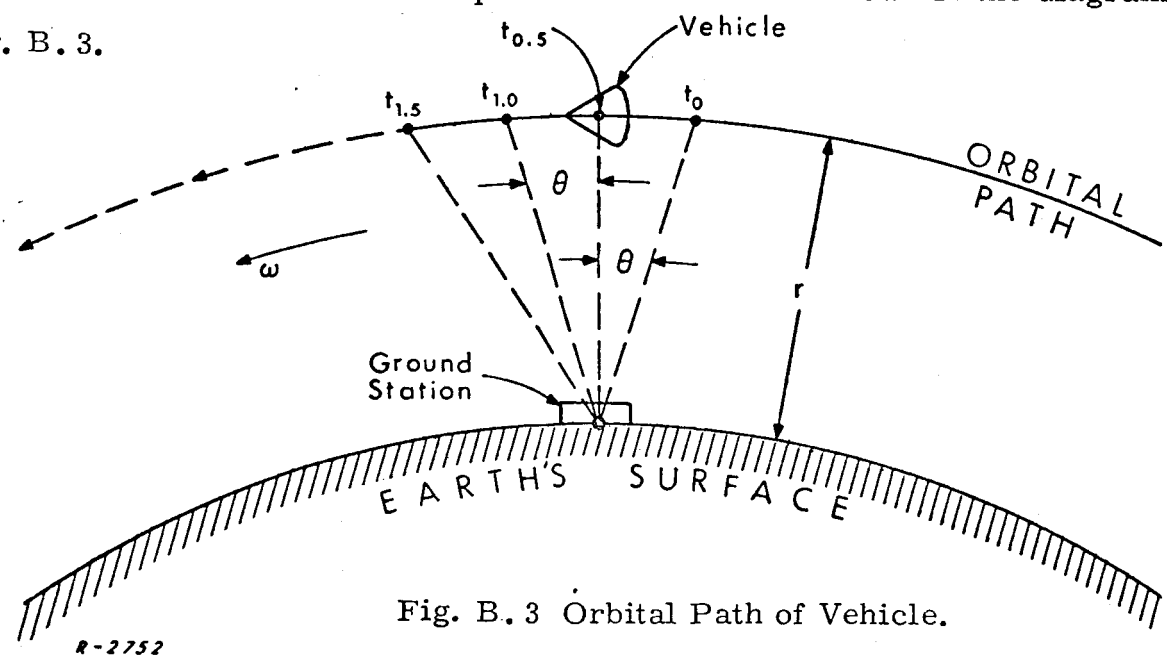


Fig. B.3 Orbital Path of Vehicle.

*i.e., one with low loss characteristics

From the AROD system specifications, the maximum vehicle velocity $v_{max}$ that the system is required to handle is 12,000 meters per second. The minimum range $r_{min}$ over which the system is required to operate is 100 km. Thus, the maximum rate of change $\omega_{max}$ of cℓ or cm which could be expected is approximately:

$$\omega_{max} \approx \frac{v_{max}}{r_{min}} = 0.12 \text{ rad/sec}$$

$$= 6.87 \text{ degrees/sec} \qquad \text{(B.1)}$$

B.2 Transient Error Following Signal Acquisition

For computation of the transient error immediately following the acquisition* of a signal, the maximum possible offset of cℓ or cm (with respect to the ambient charge on the filter capacitor) is assumed.

The charge on the filter capacitor due to a step input in voltage is given by the following equation:

$$e_2(t) = e_1\left(1 - e^{\frac{-t}{\tau}}\right) \qquad \text{(B.2)}$$

where:

$e_2(t)$ = filter output, degrees**

$e_1$ = amplitude of filter input, degrees**

$t$ = time, seconds

$\tau$ = RC = filter time constant, seconds

*The term "acquisition," as used here, is defined to mean the first instant of reception of a signal wherein the input level is such that extraction of useful information by the phase meter is possible.

**For convenience in notation, input and output voltages of the post-detection filter will be expressed directly in "degrees," since these potentials are analogs of angular direction cosines differing from the voltage values by only a scaler factor.

The lag error $\eta_A$ after a time interval t = T between the actual value of $c\ell$ or cm and the filter output is given by:

$$\eta_A = e_2(T) - e_1(T) = - E_1 \, e^{-\frac{T}{\tau}} \qquad \text{(B. 3)}$$

A plot of filter lag error $\eta_A$ as a function of the filter time constant $\tau$ is shown in Fig. B. 4. A maximum initial offset (between received signal and ambient filter capacitor charge) of 180 degrees is assumed.* Integration time or sample time T is 0. 5 second.

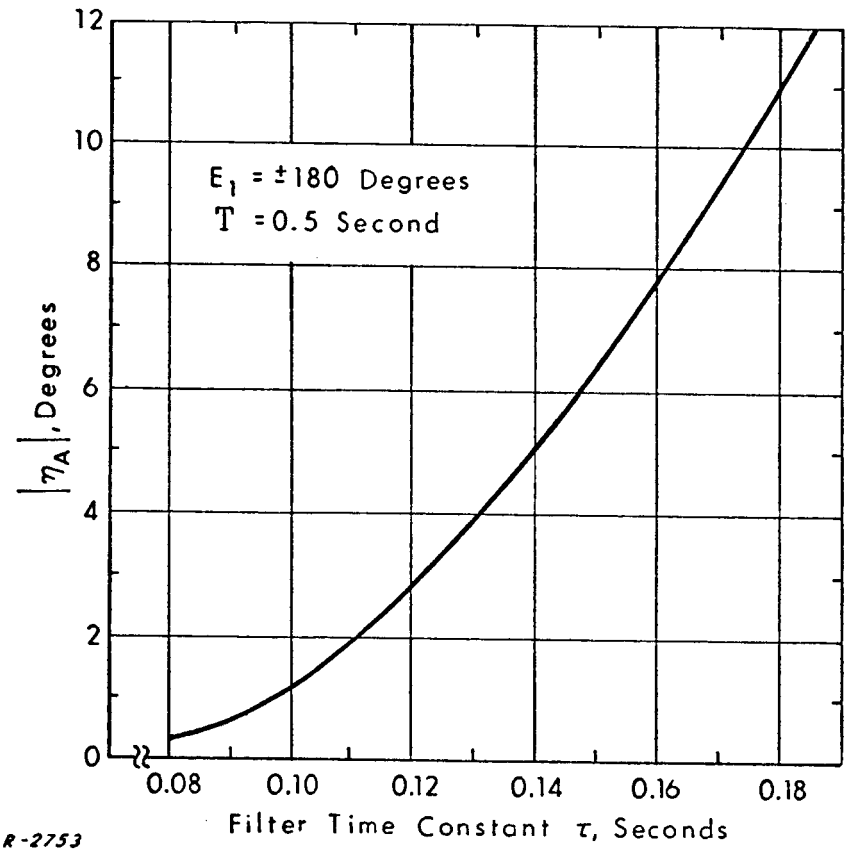


Fig. B. 4 $|\eta_A|$ as a Function of Filter Time Constant $\tau$ for a Sample Time T = 0. 5 Second.

*$\eta_A$ is proportional to initial offsets less than 180 degrees.

B. 3 Error Due to Vehicle Dynamics

The maximum filter lag error due to vehicle dynamics is a function of the filter time constant and the maximum rate of change of cℓ and cm. $\omega_{max}$ was calculated in Eq. (B. 1) to be approximately 6. 8 degrees per second. For simplicity this rate of change is assumed to be linear. Thus:

$$e_1(t) = 6.8\,t \qquad t \geq 0$$
$$= 0 \qquad t = 0 \qquad \text{(B. 4)}$$

For computational simplicity the assumption is also made that the initial capacitor charge is zero. Figure B. 5 shows the rate of change in cℓ or cm, and the corresponding charge on the filter capacitor.*

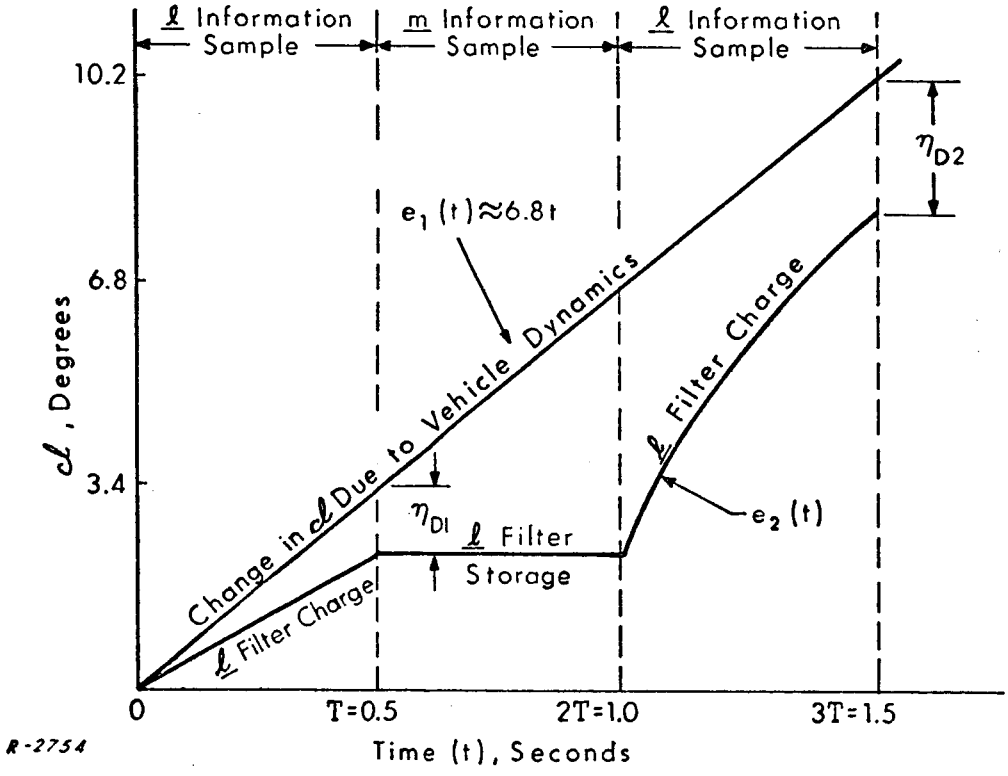


Fig. B. 5 ℓ Filter Capacitor Charge as a Function of a Change in cℓ

*Figure B. 5 shows the charge on the ℓ filter capacitor. An identical charge function exists for the m filter capacitor for a similar rate of change of cm.

The time constant $\tau$ of either filter shown in Fig. B. 2 is defined to be:

$$\tau = RC \tag{B. 5}$$

From the circuit of Fig. B. 2:

$$Z(s) = R + \frac{1}{sC} \tag{B. 6}$$

$$I(s) = \frac{E_1(s)}{R + \frac{1}{sC}} \tag{B. 7}$$

$$E_2(s) = \frac{I(s)}{sC} = \frac{E_1(s)}{s\tau + 1} \tag{B. 8}$$

The Laplace transform of Eq. (B. 4) is:

$$E_1(s) = \frac{6.8}{s^2} \tag{B. 9}$$

Therefore:

$$E_2(s) = \left[\frac{6.8}{\tau}\right]\left[\frac{1}{s^2(s + \frac{1}{\tau})}\right] \tag{B.10}$$

$$= 6.8\left[\frac{1}{s^2} - \frac{\tau}{s} + \frac{\tau}{s + \frac{1}{\tau}}\right] \tag{B.11}$$

Converting Eq. (B. 11) to the time domain:

$$e_2(t) = 6.8\left[t - \tau\left(1 - e^{\frac{-t}{\tau}}\right)\right] \tag{B.12}$$

The filter lag error $\eta_{D1}$ due to vehicle dynamics is, at t = T second:

$$\eta_{D1} = e_1(T) - e_2(T) \tag{B.13}$$

$$= 6.8\tau\left(e^{\frac{-0.5}{\tau}} - 1\right) \quad \text{for } T = 0.5 \tag{B.14}$$

At $t = 2T$, when the filter again starts to charge, there is an initial charge of $(6.8T - \eta_{D1})$ on the filter capacitor.

To solve for the filter output $e_2(t)$ in the interval $2T < t \leq 3T$ we have the initial condition

$$e_2(2T) = 6.8T - \eta_{D1} \tag{B.15}$$

and the input $e_1'(t')$ for the corresponding interval is (see Fig. B.5)

$$\begin{aligned} e_1'(t') &= 6.8(t' + 2T) \qquad t' > 0 \\ &= 0 \qquad\qquad\quad t' \leq 0 \end{aligned} \tag{B.16}$$

where $t' = (t - 2T)$. The resulting output $e_2(t)$ is thus being obtained by computing the response of the filter to the input given by Eq. (B.16) and the initial capacitor charge of (B.15). The response $e_2'(t')$ to the above conditions is given as the inverse transform of

$$\mathcal{L}\left[e_2'(t')\right] = 6.8\left\{\frac{1}{s^2} + \frac{2T}{s}\right\}\frac{1}{s\tau + 1} + (6.8T - \eta_{D1})\frac{1}{s\tau + 1} \tag{B.17}$$

where the effect of the initial condition on the filter capacitor is included as an impulse input occurring at $t' = 0$. The inverse transform of Eq. (B.17) is

$$\begin{aligned} e_2'(t') &= 6.8\left[t' - \tau\,(1 - e^{-t'/\tau})\right] + 13.6\,T(1 - e^{-t'/\tau}) \\ &\quad + (6.8T - \eta_{D1})\,e^{-t'/\tau} \\ &= 6.8t' + 13.6T - 6.8\tau(1 - e^{-t'/\tau}) - (6.8T + \eta_{D1})\,e^{-t'/\tau} \end{aligned} \tag{B.18}$$

The total error $\eta_{D2}$ is then

$$\eta_{D2} = e_1(3T) - e_2'(T) = e_1(3T) - e_2(3T) \qquad \text{(B.19)}$$

$$= (1 - e^{-T/\tau})\,\eta_{Di} - 6.8T\,e^{-T/\tau}$$

$$= -\frac{\eta_{D1}^2}{6.8\tau} - 6.8T\,e^{-T/\tau} \qquad \text{(B.20)}$$

Both these error coefficients $|\eta_{D1}|$ and $|\eta_{D2}|$ are plotted in Fig. B.6 as a function of $\tau$.

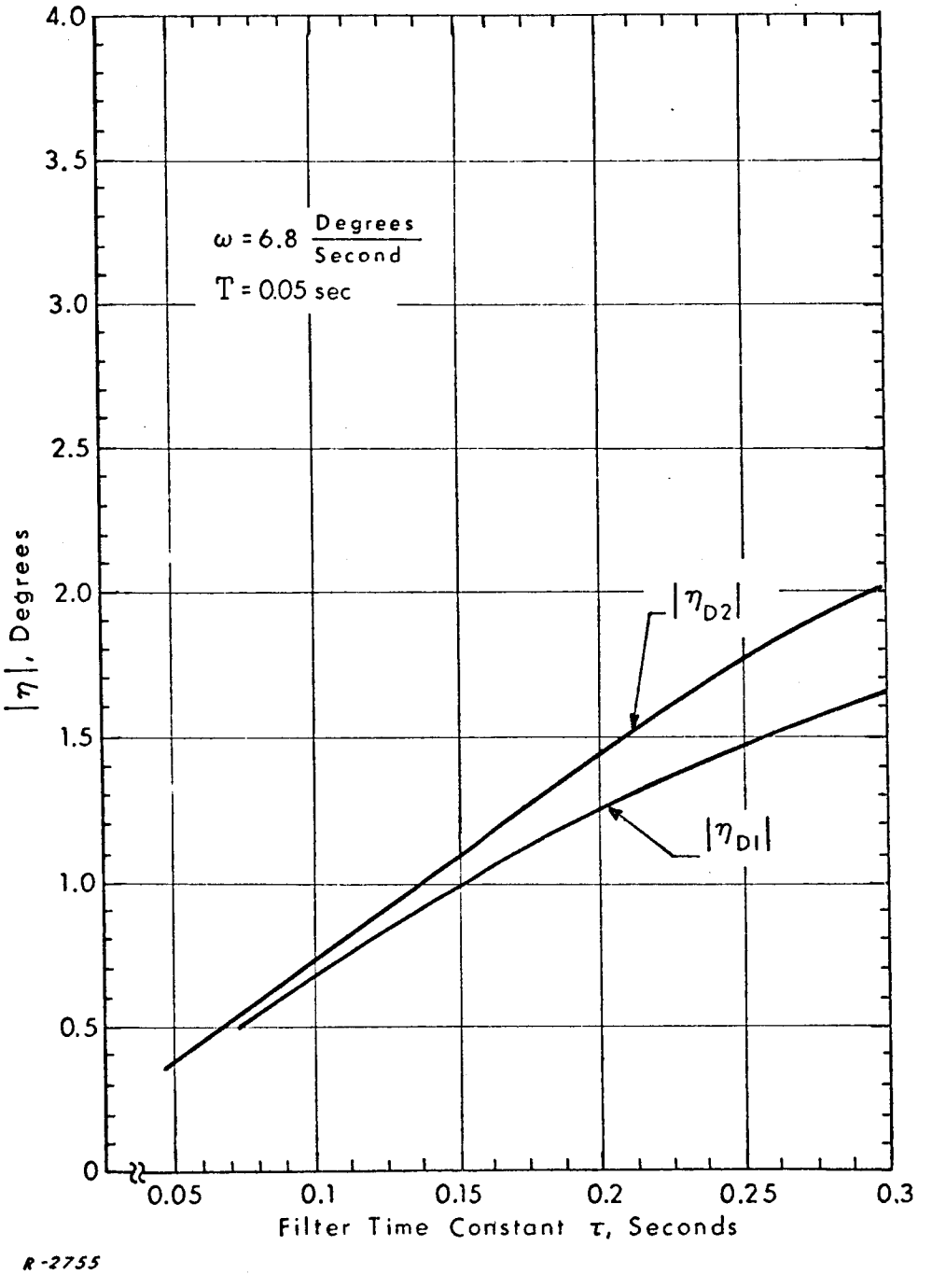


Fig. B.6 Filter Lag Error $\eta$ due to Vehicle Dynamics-Plotted as a Function of Filter Time Constant $\tau$.